

Accepted Manuscript

Genetic analysis of the wild strawberry (*Fragaria vesca*) volatile composition

María Urrutia, José L. Rambla, Konstantinos G. Alexiou, Antonio Granell, Amparo Monfort



PII: S0981-9428(17)30342-X

DOI: [10.1016/j.plaphy.2017.10.015](https://doi.org/10.1016/j.plaphy.2017.10.015)

Reference: PLAPHY 5027

To appear in: *Plant Physiology and Biochemistry*

Received Date: 15 August 2017

Revised Date: 13 October 2017

Accepted Date: 17 October 2017

Please cite this article as: Mari. Urrutia, José.L. Rambla, K.G. Alexiou, A. Granell, A. Monfort, Genetic analysis of the wild strawberry (*Fragaria vesca*) volatile composition, *Plant Physiology et Biochemistry* (2017), doi: 10.1016/j.plaphy.2017.10.015.

This is a PDF file of an unedited manuscript that has been accepted for publication. As a service to our customers we are providing this early version of the manuscript. The manuscript will undergo copyediting, typesetting, and review of the resulting proof before it is published in its final form. Please note that during the production process errors may be discovered which could affect the content, and all legal disclaimers that apply to the journal pertain.

21 **Abstract:**

22 The volatile composition of wild strawberry (*Fragaria vesca*) fruit differs from that of
23 the cultivated strawberry, having more intense and fruity aromas. Over the last few
24 years, the diploid *F. vesca* has been recognized as a model species for genetic studies of
25 cultivated strawberry (*F. x ananassa*), and here a previously developed *F. vesca*/*F.*
26 *bucharica* Near Isogenic Line collection (NIL) was used to explore genetic variability
27 of fruit quality traits. Analysis of fruit volatiles by GC-MS in our NIL collection
28 revealed a complex and highly variable profile. One hundred compounds were
29 unequivocally identified, including esters, aldehydes, ketones, alcohols, terpenoids,
30 furans and lactones. Those in a subset, named key volatile compounds (KVCs), are
31 likely contributors to the special aroma/flavour of wild strawberry. Genetic analysis
32 revealed 50 major quantitative trait loci (QTL) including 14 QTL for KVCs, and one
33 segregating as a dominant monogenetic trait for nerolidol. The most determinant
34 regions affecting QTLs for KVCs, were mapped on LG5 and LG7. New candidate
35 genes for the volatile QTL are proposed, based on differences in gene expression
36 between NILs containing specific fragments of *F. bucharica* and the *F. vesca* recurrent
37 genome. A high percentage of these candidate genes/alleles were colocalized within the
38 boundaries of introgressed regions that contain QTLs, appearing to affect volatile
39 metabolite accumulation acting in *cis*. A NIL collection is a good tool for the genetic
40 dissection of volatile accumulation in wild strawberry fruit and a source of information
41 for genes and alleles which may enhance aroma in cultivated strawberry.

42

43

44 **Keywords:** *Fragaria vesca*, volatilome, wild aroma, key volatile compounds, QTL,
45 introgression

46

47 Introduction

48 Around the past 30 years, strawberry breeding programs have been directed mainly
49 towards improving agronomical performance, resulting in varieties which produce high
50 yields of large red and firm fruits, but fruit aroma is the quality trait with a major impact
51 in consumers (Bruhn *et al.* 1991; Schwiterman *et al.* 2014). Over 350 volatile
52 compounds have been identified in fruits of *Fragaria* sp., comprising esters, aldehydes,
53 ketones, furanones, alcohols and terpenoids (Latrasse 1991) but only a few have been
54 reported to contribute to the strawberry aroma as perceived by humans (Schieberle &
55 Hofmann 1997; Ulrich *et al.* 1997; Ulrich *et al.* 2007).

56 As with other fruit crops, the biosynthetic pathways, enzymes and regulation underlying
57 volatile compound accumulation have been partially elucidated in *Fragaria*. Fruit
58 volatile profiles are known to depend on genetic (fruit species and variety),
59 developmental (maturity stage) and postharvest factors, as well as on the analytical
60 technique used. Generally, strawberry fruit volatiles increase with ripening (Goff &
61 Klee 2006) and are classified in three main categories according to their carbon source:
62 fatty acid, amino acid, and carbohydrate derivatives (reviewed by Schwab *et al.* 2008;
63 Granell & Rambla 2013).

64 Fatty acids are the most important precursors for most fruit aroma volatiles, including
65 straight-chain aldehydes, alcohols, esters, lactones and ketones. These compounds are
66 synthesized mainly through the lipoxygenase (LOX) pathway and α - β -oxidation. In the
67 LOX pathway, linoleic (18:2) and linolenic (18:3) acid are converted to hydroperoxide
68 isomers, which are then cleaved by hydroperoxide lyase (HPL) to form hexanal and (Z)-
69 3-hexenal, respectively. The aldehydes are subsequently reduced to the corresponding
70 C₆ alcohols by alcohol dehydrogenase (ADH). Alcohol acyl transferase (AAT)
71 catalyzes the reaction between an acyl moiety and an alcohol to form an ester. It has
72 been proposed that this pathway requires a still-unidentified lipase (Schwab *et al.* 2008;
73 Granell & Rambla 2013). Fatty acids can also be degraded via α - and β -oxidation
74 pathways, although the specific mechanisms in plants are not well understood. In
75 strawberry, alcohol acyl transferases (SAAT) with high sequence similarity but different
76 substrate preferences have been identified: AAT in *F. x ananassa* (SAAT, Aharoni *et al.*
77 *al.* 2000) and *F. vesca* (VAAT, Beekwilder *et al.* 2004). Additionally, an omega-6 fatty
78 acid desaturase (*FaFAD*) has been correlated with the presence of γ -decalactone
79 (Chambers *et al.* 2014; Sanchez-Sevilla *et al.* 2014).

80 Amino acid metabolism is known to be an important source of aroma volatile
81 precursors. This is the case of phenylpropanoid and benzenoid volatiles that derive from
82 phenylalanine. In strawberry, eugenol biosynthesis is mediated by two eugenol
83 synthases (*FaEGS1* and *FaEGS2*) and controlled by one R2R3 MYB transcription
84 factor (*FaEOB1*) (Aragüez *et al.* 2013; Medina-Puche *et al.* 2015). The biosynthetic
85 pathways of other volatile benzenoids have not yet been clearly elucidated. Other
86 branched-chain organic acids and aromatic amino acids are volatile precursors, however
87 their catabolic pathways to form volatile compounds also remain unclear (Granell &
88 Rambla 2013).

89 Carbohydrates can give rise directly to volatile furanones, without degradation of the
90 carbon skeleton. In *F. x ananassa*, the FaOMT enzyme transforms furaneol to
91 mesifurane (Zorrilla-Fontanesi *et al.* 2012). Volatile terpenoids (mainly mono- and
92 sesqui- terpenoids) are formed from the basic C₅ precursors isopentenyl pyrophosphate
93 (IPP) and its isomer, dimethylallyl pyrophosphate (DMAPP). IPP and DMAPP derive
94 from either the plastidic methylerythriol phosphate or the cytosolic mevalonate
95 pathway. These C₅ units are condensed to pyrophosphate precursors of terpenoids that
96 are converted to final products by terpene synthases (TPS) (Granell & Rambla 2013). In
97 strawberry, the production of the monoterpene linalool and the sesquiterpene
98 nerolidol, and that of the monoterpene α -pinene, have been shown to be linked to
99 specific alleles of the terpene synthases *FaNES1* and *FvPINS* respectively (Aharoni *et*
100 *al.* 2004).

101 Major differences in volatile patterns have been observed among different species
102 within the *Fragaria* genus. The most common volatile compounds contributing to
103 strawberry aroma are esters with methyl butanoate, ethyl butanoate, butyl butanoate,
104 methyl hexanoate, ethyl hexanoate, butyl acetate and hexyl acetate as important
105 contributors to the fruity aroma. Methyl 2-aminobenzoate (also known as methyl
106 anthranilate) has been reported as the single compound which confers the typical “wild
107 strawberry-like” aroma of woodland strawberry (*F. vesca*) accessions, and is only very
108 rarely found in some commercial varieties (Ulrich *et al.* 1997). Methyl cinnamate adds
109 spicy notes and myrtenyl acetate herbaceous notes (Schieberle & Hofmann 1997; Ulrich
110 *et al.* 1997; Jetty *et al.* 2007; Ulrich *et al.* 2007; Olbricht *et al.* 2008; Schwieterman *et al.*
111 2014). Furans, specifically furaneol and mesifurane, are considered important
112 contributors by adding caramel notes (Schieberle & Hoffmann 1997, Ulrich *et al.* 1997;
113 Ulrich *et al.* 2007; Jetty *et al.* 2007), while the terpenoids linalool and nerolidol, add

114 flowery notes (Ulrich *et al.* 1997, Olbrich *et al.* 2008, Schwieterman *et al.* 2014), but
115 these compounds have been detected mainly in octoploid cultivars (*F. x ananassa*) and
116 not in diploid wild strawberries (*F. vesca*) (Aharoni *et al.* 2004). The so-called ‘green
117 volatile compounds’, (*Z*)-3-hexenal, (*E*)-2-hexenal and (*Z*)-3-hexen-1-ol, have been
118 reported to contribute to the aroma characteristics that typically decrease with ripening
119 (Ulrich *et al.* 1997, Schieberle & Hoffman 1997). Another important volatile compound
120 is γ -decalactone, which confers ‘peach-like’ notes (Ulrich *et al.* 1997, Jetty *et al.* 2007,
121 Olbrich *et al.* 2008).

122 A distinctive characteristic of volatile composition in *F. vesca* fruit is that it is richer in
123 esters and monoterpenes (α -pinene, β -myrcene, α -terpineol, α -phellandrene) while
124 exhibiting the pleasant and easily identifiable ‘wild-strawberry-like’ aroma associated
125 with methyl 2-aminobenzoate. These compounds confer more intense and fruity aroma
126 characteristics of this wild species and are not found normally in commercial strawberry
127 fruits (*F. x ananassa*) (Aharoni *et al.* 2004, Ulrich *et al.* 1997; Ulrich *et al.* 2007; Dong
128 *et al.* 2013). It is important to emphasize that large differences have been observed
129 between *F. x ananassa* varieties covering a range of fruit quality phenotypes (Zorrilla-
130 Fontanesi *et al.* 2012; Schwieterman *et al.* 2014).

131 To date, research has been directed to the characterization of the aroma profile of
132 different octoploid accessions, mapping populations resulting from crosses involving
133 commercial and wild material (Jetty *et al.* 2007; Olbricht *et al.* 2008; Zorrilla-Fontanesi
134 *et al.* 2012; Schwieterman *et al.* 2014), and differences in the aroma profiles between
135 octoploid and diploid strawberries (Aharoni *et al.* 2004; Ulrich *et al.* 2007; Dong *et al.*
136 2013). It is surprising that, despite the outstanding organoleptic characteristics of *F.*
137 *vesca*, the genetic basis of its characteristic volatile content have not been yet reported.
138 Given the very high degree of synteny between *F. vesca* and the commercial hybrid *F. x*
139 *ananassa* (Rousseau-Gueutin *et al.* 2008, Tennessen *et al.* 2014), *F. vesca* is a model for
140 the study of strawberry genetics what facilitates the transfer of information and alleles
141 to modern varieties. In addition, the high quality reference genome sequence available
142 (Shulaev *et al.* 2011), the transcriptomic analysis re-annotation of the species (Darwish
143 *et al.* 2015) and the recently developed near isogenic line (NIL) mapping collection
144 (Urrutia *et al.* 2015) are powerful tools for the study of genetic traits in strawberry.
145 Specifically, strawberry NIL collection derived from an inter-specific cross between *F.*
146 *vesca* and *F. bucharica*. The homozygous introgressions of *F. bucharica*, an exotic

147 relative of *F. vesca*, give phenotypic variability that has been used to map QTL for
148 agronomical and metabolic traits (Urrutia *et al.* 2016).

149 This study provides a detailed profiling and QTL mapping of the volatile composition
150 of a *F. vesca* NIL population, as a first step to identifying the genetic basis of the wild
151 strawberry-like aroma. We focused on two genome regions that harbor key aroma
152 volatile QTL, a whole transcriptomic study of the corresponding lines allowed us to
153 select a number of differentially expressed candidate genes as responsible for the
154 differences in volatile accumulation.

155

156 **Materials and Methods**

157 Plant material and sample extraction

158 The volatilome of diploid strawberry ripe fruits was analyzed using 42 lines from a near
159 isogenic line (NIL) collection in *F. vesca*, its recurrent and donor parents (*F. vesca* var.
160 ‘Reine des Vallées’ and *F. bucharica* ‘FDP 601’ respectively) and the yellow-fruited
161 variety of *F. vesca* named ‘Yellow Wonder’ (YW), which has a very pleasant
162 pineapple-like aroma. Each line was represented by six to eight individuals
163 independently grown from seed in two different years (2012 and 2013) and cultivated in
164 a shaded greenhouse in Caldes de Montbui (latitude: 41° 36’N, longitude: 2° 10’ E,
165 altitude 203m above sea level, pre-coastal Mediterranean climate) following the usual
166 agronomical practices for this crop. Pools of berries from each genotype were collected
167 at harvest time and immediately frozen in liquid nitrogen as independent biological
168 replicates. Three to five biological replicates were harvested, ground to fine powder and
169 stored at -80°C prior to gas chromatography-mass spectrometry (GC-MS) analysis
170 and/or total RNA extraction. The NIL collection is extensively described in Urrutia *et*
171 *al.* (2015).

172

173 Volatile compounds analysis

174 Volatile compounds were determined in a similar way as described in Rambla *et al.*
175 (2015). Each biological replicate was analyzed as an independent sample. Before the
176 volatile compounds analysis, an aliquot of 500 mg of frozen fruit powder from each
177 sample was weighed in a 7 mL glass vial and thawed at 30°C for 5 min. Then 500 µL of
178 a saturated NaCl solution were added and the mixture was homogenized gently. Five
179 hundred microliters of the resulting paste were transferred to a 10 mL screw cap
180 headspace vial and analyzed immediately. Volatiles were sampled by HS-SPME
181 (headspace solid phase microextraction) with a 65 µm PDMS/DVB
182 (polydimethylsiloxane/divinyl-benzene) fiber (Supelco, PA, USA). The vials were first
183 tempered at 50°C for 10 min, then volatiles were extracted by exposing the fiber to the
184 vial headspace for 30 min at 50°C with agitation at 500 rpm. The extracted volatiles
185 were desorbed in the GC injection port at 250°C for 1 min in splitless mode. A Combi-
186 PAL autosampler (CTC Analytics, Zwingen, Switzerland) was used for incubation,
187 volatile extraction and desorption. GC-MS was in a 6890N gas chromatograph coupled
188 to a 5975B mass spectrometer (Agilent Technologies, CA, USA). A DB-5ms column
189 (60 m, 0.25 mm, 1 µm) (J&W Scientific, CA, USA) and a constant helium flow of 1.2

190 mL min⁻¹ were used for chromatographic separation. Oven programming conditions
191 were: 40°C for 2 min, 5°C min⁻¹ ramp to 250°C, then 5 min at 250°C. Compounds were
192 monitorized over the mass/charge ratio (m z⁻¹) range of 35-250. Chromatograms and
193 mass spectra were analyzed using the Enhanced ChemStation software (Agilent
194 Technologies, CA, USA). Volatile compounds were unambiguously identified by
195 comparison of both retention time and mass spectra to those of commercial standards
196 (SIGMA-Aldrich, MO, USA) run under the same conditions, except four compounds
197 which were tentatively identified by comparison of their mass spectra to those in the
198 NIST 05 mass spectral library. These compounds are marked with a “T” after the
199 chemical name (Table 1). For quantification, a specific ion was selected for integration
200 of the area of each of the identified compounds. Areas were normalized by comparison
201 with the peak area of the same compound in a reference sample which was injected
202 regularly each five to six samples, in order to correct for variations in sensitivity and
203 fiber aging. This reference sample consisted of a homogeneous mix of all the samples
204 analyzed each year.

205

206 Data and mQTL analysis

207 Volatiles are expressed in relative terms, as a ratio between each sample and a quality
208 control sample (a mix of all studied samples) to correct for technical drift. In order to
209 assess normality for statistical data analysis, ratios were transformed to base 2
210 logarithm. All the lines that set fruit were processed and analyzed by GC-MS each year
211 (Supplemental Table 1). However, for the exploratory analysis, only those genotypes
212 that produced enough fruits both years were considered (Urrutia et al 2016). For the
213 statistical analysis and graphical representations, the free source software R 2.15.1
214 (RCoreTeam, 2012) was used, with the Rstudio 0.92.501 interface (Rstudio, 2012)
215 unless otherwise specified. Pearson’s correlation was calculated using the *rcorr* function
216 from the *Hmisc* package (Harrell, 2014). The *Anova* function from the *car* package (Fox
217 2011) was used for analysis of variance (ANOVA). Omega squared values (ω^2) were
218 calculated from ANOVA residuals following the formula: $(SS_i - df_i * MS_{err}) * (MS_t +$
219 $MS_{err})^{-1}$. For Principal Components Analysis (PCA), the *prcomp* function and scaled
220 values were used. The Hierarchical Clustering Analysis (HCA) was calculated
221 considering Euclidean distance and the complete linkage clustering method. The Cluster
222 Network Analysis (CNA) was calculated with the *qgraph* function from the *qgraph* R
223 package (Epskamp et al. 2012). Significance tests were recursively calculated between

224 each NIL and RV ratio using the *t.test* function and corrected for multi-testing by
225 *p.adjust* (threshold *p. adjusted* < 0.05) for QTL mapping. QTLs were mapped to a
226 specific genetic region only when all NILs harboring a common *F. bucharica*
227 introgression in this region showed a significant effect and in the same direction over
228 the ratio for the specific metabolite of study. QTL that were mapped to the same region
229 in two harvests were considered stable. Interval mapping analysis with MapQTL v.6
230 (Van Ooijen 2009) was used to confirm these QTL and estimate their effect. Stable
231 QTL that explained around 20% or more of the variability and had LOD scores >1.8
232 were considered major QTLs. Non-stable QTL (detected in only one harvest) were
233 considered only if they accounted for more than 20% of the observed variability that
234 year. Graphical representation of the mQTLs was using MapChart 2.2 (Voorrips, 2002).

235

236 RNA sequencing and analysis

237 Total RNA was isolated from three selected NILs (Fb5:0-35 and Fb7:0-10) and the
238 recurrent parental (RV) extracting the nine samples (three biological replicates per line)
239 following the protocol described by Liao *et al.* 2004. A cell lysis step with CTAB
240 buffer, modified with 3% PVP and 4% β -mercaptoethanol, was followed by: 2-3
241 cleaning steps with chloroform-isoamyl alcohol (24:1 v/v), overnight precipitation with
242 lithium chloride (8 M), 1-2 additional cleaning steps with chloroform-isoamyl alcohol
243 (24:1 v/v) and precipitation with cold absolute ethanol. RNA was quantified and
244 checked for purity and integrity in a Bioanalyzer-2100 (Agilent Technologies, CA,
245 USA). The concentration and quality threshold was set at 150 ng/?L and RNA integrity
246 number (RIN) above eight. Further steps in RNA quality control, library preparation
247 and mRNA paired end (2 x 75bp) sequencing were carried out at the Centro Nacional de
248 Análisis Genómico (CNAG), Spain in a HiSeq2000 sequencer (Illumina, CA, USA).
249 For quality control, trimming of sequencing adapters and removal of low quality and
250 short reads (<40bp), FASTQC v0.10.1

251 (<http://www.bioinformatics.babraham.ac.uk/projects/fastqc>) and Trimmomatic v0.32
252 (Bolger *et al* 2014) were used respectively. Trimmed reads were mapped against the
253 *F. vesca* reference genome v1.1 using Tophat v2.0.11 with default parameters (Trapnell
254 *et al.* 2009), taking as annotation reference version 2 (a2) (Darwish *et al.* 2015) and
255 version 1 (a1) (<https://www.rosaceae.org/species/fragaria/fragaria-vesca>). Mapping
256 quality was evaluated with the *bamqc* and *rnaseq* functions from Qualimap v2.1
257 (García-Alcalde *et al* 2012).

258

259 Differential gene expression analysis and functional annotation

260 Differential expression analysis was first performed using annotations a2 and then
261 complemented, using the same filters and parameters, with a1. Independent tables of
262 counts per gene were first generated with *HTSeq-count* with mode *union* (Anders et al
263 2014), considering all annotated genes from the reference annotation a2 and a1
264 respectively. These tables were provided as input to the DESeq package in R (Anders
265 and Hubers 2010) using the *newCountDataSetFromHTSeqCount* function. DESeq
266 counts all the reads-pairs mapped to a gene and normalizes the number of counts
267 between samples, correcting for the library size. We considered that a gene was
268 expressed in a specific line if at least two of the three biological replicates had ≥ 1
269 read-counts for the gene. Secondly, 40% of the genes with lowest standard deviation
270 were filtered in order to maximize the discovery rate. Differential expression analyses
271 contrasting each NIL against RV were computed with the *nbinomTest* function (Anders
272 and Hubers 2010). Multi-testing corrected p-values (p-adjust) were calculated using the
273 Benjamini & Hochberg method. The significance threshold for a differentially
274 expressed gene (DEG) was fixed at p-adjust=0.1. Lists of DEGs obtained with a2
275 (Supplemental Table 6) and a1 were compared for coincidence. DEG lists were inquired
276 for predicted protein similarity with other proteins annotated in plant databases. The
277 mRNA sequence was extracted from predicted exon coordinates. These mRNA
278 sequences were inquired by *blastx* with the *GoAnna* tool from Agbase (McCarthy et al
279 2006) against the manually annotated protein plant database, with a significance
280 threshold of 0.05. Annotated function and gene ontology terms (GO terms) of best blast
281 hits were assumed as putative functions by mRNA query. In order to obtain a
282 summarized view of the functional annotation results we used *GoSlimViewer* from
283 AgBase (McCarthy et al 2006). In addition, functional enrichment analysis to detect
284 metabolic functions or biological processes that might be over-represented among the
285 DEGs was carried out using the MetGenMAP online platform (Joung et al 2009).
286 Putatively affected metabolic pathways were also explored using MetGenMAP.

287

288 Variation calling

289 SNP and INDEL detection was only carried out for the genomic regions where an
290 introgression of *F. bucharica* was present. Alignment files generated by TopHat for
291 each NIL were indexed and then filtered to contain reads mapping to the respective *F.*

292 *bucharica* introgressed regions, using Samtools (v1.2.0). Further filtering of the
293 alignment files included removal of duplicate reads (“samtools rmdup”) and additional
294 steps as described in the “GATK Best Practices workflow for SNP and indel calling on
295 RNAseq data” (GATK-3.1.1;
296 <https://www.broadinstitute.org/gatk/guide/article?id=3891>). Briefly, after removal of the
297 duplicate reads, sequences overhanging the intronic regions were hard-clipped using
298 '*SplitNCigarReads*', mapping qualities (MAPQs) reassigned using '*PrintReads*' and local
299 INDEL realigned using '*RealignerIndelCreator*' and '*IndelRealigner*'. Clean and
300 reformatted alignment files were used as input for variant calling with Samtools (v1.2.0)
301 using default parameters, except for applying a downgrading of mapping quality for
302 reads containing excessive mismatches (-C 50).

303 **Results**304 Variability in the profile of fruit volatile compounds in the strawberry NIL collection

305 In order to detect genetic regions affecting wild strawberry aroma, differences in
306 volatile accumulation were evaluated over two years in ripe fruit of NILs derived from
307 an interspecific *Fragaria* cross (*F. vesca* var. 'Reine des Vallées' (RV) as recurrent
308 parent x *F. bucharica* 'FDP601' (FB), as donor parental; Urrutia *et al.* 2015). Fruits
309 from the RV were used as a reference for the changes in volatiles observed in the
310 population, and fruit from the aromatic white-fruited *F. vesca* var. Yellow Wonder
311 (YW) were used as an external control or out-group. Metabolite profiling by GC-MS
312 analyses and QTL mapping were performed with all the genotypes that set enough fruit
313 each year, but we only considered those that were represented by at least three
314 biological replicates in both years for the statistical analysis (i.e. 25 genotypes,
315 Supplemental Table 1).

316

317 We were able to identify 100 volatile compounds, 96 of which were unambiguously
318 identified by comparison of both retention time and mass spectra with those of
319 commercial standards run under the same conditions, whilst the remaining four
320 compounds were tentatively identified based on their mass spectra (these are marked
321 with a T at the end of the chemical name, see Table 1). The unequivocally identified
322 volatile compounds were 11 alcohols, 16 aldehydes, 46 esters, four furans, 14 ketones,
323 eight terpenoids and one lactone, and include most of the compounds described in the
324 literature as contributing to strawberry aroma (Schieberle & Hofmann 1997; Ulrich *et*
325 *al.* 1997; Ulrich *et al.* 2007). Here we refer to them as 'key volatile compounds'
326 (KVCs), and have marked them with an arrow symbol in Table 1. KVCs that confer
327 specific strawberry aroma are 12 esters butyl acetate, butyl butanoate, (E)-2-hexenyl
328 acetate, ethyl butanoate, ethyl hexanoate, hexyl acetate, methyl-2-aminobenzoate,
329 methyl butanoate, methyl cinnamate, methyl hexanoate, myrtenyl acetate and (Z)-3-
330 hexenyl acetate; two aldehydes (E)-2-hexenal and (Z)-3-hexenal; two furans furaneol
331 and mesifurane; two terpenoids linalool and nerolidol, and one lactone γ -decalactone.

332

333 The relative levels (see M&M) for most volatile compounds had mean ratios around one
334 for RV in both harvests (Table 1) consistent with the nearly isogenic nature of the NIL
335 collection, which means lines share much of the common RV genetic background. The
336 variation interval for each volatile (min. and max. ratio) show different ranges of

337 variation in the NIL indicating that genes involved in accumulation of the volatile
338 compounds segregated in our NIL collection. More extreme values were detected for
339 the lower than for the higher ratios, indicating that, globally, *F. bucharica* alleles
340 decrease volatile accumulation of *Fragaria* berries. Different degrees of variation were
341 detected depending on the volatile, with decanal (4-fold variation from 0.39 to 1.49 in
342 2012) and γ -decalactone (10,000-fold variation, ranging from 0.01 to 119.96 in 2013)
343 defining the extremes of the variation range. It is also noteworthy to mention that
344 nerolidol segregated as a dominant monogenetic trait in our population, with the *F.*
345 *bucharica* alleles conferring the ability to produce nerolidol in the otherwise non-
346 nerolidol producer *F. vesca* background (Supplemental Table 1). Dominance of the *F.*
347 *bucharica* nerolidol allele was determined in the F₁ fruit samples (hybrid *F. vesca* RV x
348 *F. bucharica*), which confirmed their ability to produce nerolidol (assayed in 2013
349 only).

350

351 Relations between volatile compounds and NILs

352 Each NIL had a characteristic volatile profile according to the *F. bucharica*
353 introgression, and volatile compounds could be clustered according to their levels in the
354 different NILs (Figure 1, Table 1). Volatiles with similar chemical structure or in the
355 same biosynthetic pathways tend to be co-regulated and therefore clustered together.
356 Cluster A (16 volatiles) is enriched in long carboxylesters, particularly in octyl-derived
357 esters. Cluster B (two volatiles) includes (*E*)-2-hexenyl acetate and its free alcohol (*E*)-
358 2-hexen-1-ol. Cluster C (35 volatiles) groups all the aldehydes (except (*E*)-2-decenal),
359 and terpenoids (except α -farnesene) and most C₄ alkyl acetates. Cluster D is divided in
360 two sub-clusters, D1 (7 volatiles) which is enriched in benzenoid-derived volatiles,
361 including two furans (mesifurane and furaneol), and D2 (40 volatiles), enriched in esters
362 derived from butanoic and acetic acids, long chain alcohols and ketones. Compared to
363 *F. vesca* RV, *F. vesca* YW presented quite a different volatile profile which is enriched
364 in esters (clusters A and D2) and with decreased levels of compounds in clusters B, C
365 and D1 (Figure 1). The effect of the *F. bucharica* alleles is obvious in lines with
366 introgressions at the beginning of LG3 (Fb3:0-8, Fb3:0-15). These lines are
367 characterized by an over-accumulation of the monoterpenoid linalool (96) and the
368 sesquiterpenoid nerolidol (99), which suggests a more active terpene synthase allele
369 from *F. bucharica* associated to this region. Differences were most prevalent in lines
370 with introgressions in LG5, indicating that major QTLs for volatile accumulation are

371 located in LG5. Lines carrying introgressions of *F. bucharica* in LG7 showed a
372 tendency to over-accumulating esters (cluster A) and under-accumulating of aldehydes
373 and terpenoids (cluster C). Mean ratios for all the samples analyzed each year are
374 provided in Supplemental Table 1.

375

376 The patterns of volatile accumulation were quite stable: positive Pearson's pair-wise
377 significant correlations were detected for 82 of the 100 compounds between two years
378 at p -value <0.05 (75 with an adjusted p -value <0.01). This high correlation affected all
379 KVCs except furaneol and butyl acetate (Table 1).

380

381 Compounds belonging to the same biosynthetic pathway tended to be highly correlated,
382 as can be seen by cluster network analysis (CNA) in the case of esters and alcohols,
383 fatty acid-derived and phenylalanine-derived compounds and terpenoids (Figure 2).
384 Volatiles whose biosynthetic pathways have not been elucidated, were also highly
385 correlated to other volatile metabolites, which could indicate common regulation.
386 Individual correlation coefficients and significant values are provided in Supplemental
387 Table 2.

388

389 Variability in volatile levels across the different NIL, RV and YW fruit samples was
390 also analyzed by principal component analysis (PCA) (Figure 3). PCA suggested that
391 variation of most of the volatiles is continuous, and differences in the aroma pattern
392 between the NILs were restricted to single or small subsets of metabolites. A closer look
393 to the PCA shows that NILs samples spread along PC1 according to their introgressed
394 region (Figure 3A), while PC2 divides the samples again according to their genotype
395 but also according to the harvest year, indicating that a higher proportion of the
396 observed variability between the NILs was due to genotype rather than to environmental
397 factors. This PCA also indicated that volatile accumulation in NIL with introgressions
398 in LG2 and LG3 were especially susceptible to the environmental conditions.
399 According to the corresponding loading plots (Figure 3B), linalool (96), octanal (25)
400 and 6-methyl-5-hepten-2-one (86) together with most esters and alcohols, were mostly
401 responsible for the variability along PC1. Compounds contributing mostly to variability
402 across PC2 were C₆ lipid derivatives (*E*)-2-hexenal (17), (*E*)-2-hexenyl acetate (43),
403 (*E*)-2-hexen-1-ol (9) and (*Z*)-3-hexenal (27), aldehydes (*E*)-2-nonenal (18) and (*E*)-2-

404 heptenal (16), and the terpenoid myrtenol (97). Among all the samples, YW was the one
405 with the most differentiated volatile profile.

406

407 Genotypic and environmental effect on the accumulation of volatile compounds

408 Genotypic (G) and environmental (E) effect on the volatile accumulation was evaluated
409 by analysis of variance (ANOVA) fitting the model G+E+GxE (years taken as different
410 environments). Several factor combinations influenced variability depending on the
411 given compound. G significantly contributed (p -value<0.05) to variability of 98 out of
412 the 100 studied volatile compounds (Supplemental Table 3). Among them, 33
413 compounds were significantly influenced by the three factors G, E and GxE. Sixteen
414 volatiles were mostly influenced by G and E but not by the GxE interaction, 33 were
415 influenced by G and GxE but not by E and, most interestingly, 17 volatile compounds
416 were influenced only by G, including some of the KVCs-like methyl 2-aminobenzoate,
417 nerolidol, γ -decalactone, ethyl butanoate and (*Z*)-3-hexenal. Each of the factors also
418 differs in the actual percentage of variability they account for. In general, genotype has
419 a stronger effect on volatile variability than the environment (year) or the GxE
420 interaction (Figure 4; see also Supplemental Table 3). The G factor accounted for >50%
421 of observed variability in 35 compounds (including ten KVCs: 17, 27, 39, 43, 55, 61,
422 66, 73, 96, 99), but its effect was up to 70% for six volatiles, including four KVCs ((*E*)-
423 2-hexenal, (*Z*)-3-hexenal, (*E*)-2-hexenyl acetate and linalool). The E factor was less
424 important and only surpassed 20% of the observed variability in the case of five
425 compounds (including the KVC mesifurane).

426

427 Volatile QTL analysis

428 Genetic regions controlling ripe-fruit wild strawberry volatile accumulation were
429 detected by QTL mapping. A total of 126 QTL were mapped, 102 of which were stable
430 QTL (detected in two years) and 50 of them were major QTL (stable and explaining
431 >20% of the variability and with LOD>1.8). The QTL corresponded to 81 different
432 compounds (40 esters, 12 aldehydes, 11 alcohols, eight ketones, seven terpenoids and
433 three furans). The effect of the *F. bucharica* alleles on the *F. vesca* RV genetic
434 background was positive (producing an increased volatile accumulation) in 30 of them
435 and negative (reducing their levels) in 96 of them (Table 2).

436

437 Considering the major volatile QTL, 25 corresponded to compounds that mapped to a
438 single locus. This included nine KVCs (linalool, nerolidol, mesifurane, methyl
439 hexanoate, methyl cinnamate, (*E*)-2-hexenal, (*E*)-2-hexenyl acetate, (*Z*)-3-hexenal and
440 (*Z*)-3-hexenyl acetate), and three compounds mapped to two major QTL (the KVCs
441 methyl 2-aminobenzoate, nerol and 3-methyl-2-butenyl acetate: Table 2, Figure 5).
442 Genotype had a major effect on most of the volatile compounds for which major QTL
443 were mapped, but the effect of the environment was low (Figure 4). One of the
444 exceptions was mesifurane, which, although clearly influenced by the environment
445 (38%), the effect of the genotype (30%) was enough to map a QTL. There were also
446 some compounds, mainly lipid derivatives including aldehydes (octanal, nonanal,
447 decanal, (*E*)-2-octenal, (*E*)-2-nonenal and (*E*)-2-decenal), alcohols (1-penten-3-ol, 1-
448 hexanol and 2-heptanol) and ketones (1-penten-3-one, 2-pentanone and 2-nonanone),
449 that only resulted in QTLs that could be mapped in a single year and therefore were
450 classified as not stable. Most of these compounds were highly dependent on the
451 environment, with a low correlation between harvests.

452

453 Co-localized QTL may indicate co-regulated compounds. Two regions in the wild
454 strawberry genome harbor the highest number of major volatile QTL and QTL for
455 KVCs: LG5 and LG7 (Figure 5). The central region of LG5 (LG5:11-35 cM) appears to
456 be very important for the wild strawberry aroma as it had major QTL (negative) for the
457 accumulation of nine esters, five of which were KVCs: methyl 2-aminobenzoate,
458 myrtenyl acetate, methyl butanoate, butyl butanoate and methyl hexanoate. The bottom
459 of LG5 (LG5:50-76 cM) harbors QTLs for fatty acid derived volatiles associated with
460 green-fresh aroma. Positive QTL were mapped for (*Z*)-3-hexenal and (*Z*)-3-hexenyl
461 acetate, and negative QTL for their respective trans-2 isomers (*E*)-2-hexenal and (*E*)-2-
462 hexenyl acetate. This suggests that *F. bucharica* alleles in this region reduce conversion
463 of (*Z*)-3-hexenal (synthesized from linolenic acid) to (*E*)-2-hexenal, that would lead to a
464 higher accumulation of (*Z*)-3- derivatives and a lower accumulation of (*E*)-2-
465 derivatives (Granell & Rambla 2013). In addition, three positive QTL for the terpenoid
466 nerol, the benzenoid eugenol and the aldehyde (*E*)-2-heptenal, and one negative QTL
467 for the alcohol (*E*)-2-hexen-1-ol are localized in the same region. The top region in LG7
468 also seems to be important for wild strawberry scent as it accumulated 13 major QTL,
469 two of which correspond to key aroma contributors involved in wild strawberry-like
470 aroma (methyl 2-aminobenzoate at LG7:0-10 cM) and sweet-caramel notes (mesifurane

471 at LG7:26-43 cM). Additionally, at the top of LG7:0-10 cM we found four major QTL
472 for the accumulation of long esters and two major QTL for monoterpenoids (limonene
473 and myrtenol). Another interesting genetic region for key aroma volatiles is LG3:0-
474 8 cM where two major QTL for nerolidol and linalool accumulation were mapped.
475 Nerolidol show an absence (RV alleles) - presence (FB alleles) segregating pattern.

476

477 Whole transcriptome analysis of two rich volatile QTL regions

478 The NILs Fb5:0-35 and Fb7:0-10 (with introgression sizes of 6.51 and 14.20 Mb
479 respectively) carry QTL for key volatile esters in wild strawberry aroma, namely methyl
480 2-aminobenzoate but also myrtenyl acetate, methyl butanoate, butyl butanoate and
481 methyl hexanoate. The transcriptome of ripe berries from these two NILs were analyzed
482 and compared with their recurrent parental (RV) transcriptome in order to identify
483 differences in expression of specific genes that could be linked to the observed
484 phenotypic changes. Transcriptomes were obtained by RNAseq approach using three
485 biological replicates (nine samples in total). A total of 407 million (M) read-pairs were
486 obtained with an average of 45 M read-pairs per sample (min. 33M, max. 58M). The
487 quality of raw read pairs was assessed and sequencing adapters and low quality reads
488 were filtered. A total of 374 M (92%) passed the filter cutoff and were kept for further
489 analysis (average of 41.62 M read-pairs per sample). A high percentage of reads (83-
490 86%) could be mapped to the reference *F. vesca* genome v1.1 (Supplemental Table 4).
491 According to the latest annotation version (Darwish et al. 2015), 73 to 75% of mapped
492 reads were located in exons, 9% in introns and the remaining 16 to 18% in intergenic
493 regions. Differential expression analysis between the selected NILs (Fb5:0-35 and
494 Fb7:0-10) and the recurrent parental (RV), showed that the majority of the 31,778
495 studied genes, 17,906 (56%) were similarly expressed in both NILs and RV.
496 Additionally, 2,847 genes were expressed in at least one of the lines, with 388 detected
497 only in Fb5:0-35, 663 in Fb7:0-10, and 437 detected only in RV, while 11,025 (35%)
498 were not expressed in any of the NILs nor in RV (Figure 6).

499

500 Differential expression analysis revealed 257 differentially expressed genes (DEGs)
501 between Fb5:0-35 and RV and 442 DEGs between Fb7:0-10 and RV (DEG significance
502 threshold fixed at p-value=0.1) (Table 3, Supplemental Table 5). The large majority of
503 the DEGs were altered only in one NIL with respect to *F. vesca* RV. This was expected
504 as NILs do not share overlapping introgressions. However, there were also 33 genes

505 differentially expressed in both NILs when compared with *F. vesca* RV (Figure 6).
506 Analysis of genome position showed that a high percentage of the DEGs in each NIL
507 (54% in Fb5:0-35 and 59% in Fb7:0-10) were located within the boundaries of their
508 introgressed region, indicating that they are probably acting on *cis*, that is that the
509 differences in expression and their effects are likely to be due to allelic differences of
510 the genes in the region (Figure 7).

511

512 Functional annotation of DEGs resulted in significant blast hits for around 83% of them.
513 Gene Ontology (GO) categorization for molecular function and biological process
514 indicated that 48 DEGs were annotated as involved in metabolic activity (Supplemental
515 Table 6). This suggests that *F. bucharica* introgressions are likely to affect fruit
516 metabolism.

517

518 In addition, several DEGs were predicted as being involved in known volatile synthetic
519 pathways in *F. vesca* (Table 4), such as the lipoxygenase pathway (13-LOX and 13-
520 HPL pathway) in NIL Fb7:0-10 and terpene synthesis in NIL Fb5:0-35. We carefully
521 selected candidate genes by combining expression data with the metabolic QTL (Table
522 5). The NILs Fb5:50-76 and Fb7:0-10 contain QTL for fatty-acid derived volatiles.
523 Differentially expressed lipoxygenases (4) and acyltransferases (6) were found in Fb7:0-
524 10, and one down-regulated acyl-transferase was detected in Fb5:0-35. Selected NILs
525 were also found to harbor several QTL for terpenoids that might be of interest for wild
526 strawberry aroma (Table 2). A differentially expressed sesquiterpene synthase was
527 detected in Fb5:0-35 and a terpene synthase in Fb7:0-10 (Table 5).

528

529 Several transcription factors (TF) were also differentially expressed in NIL Fb5:0-35
530 and Fb7:0-10 with respect to RV. As alterations in TF can have wide range effects, all
531 of them were considered candidate genes. A putative MYC2 TF up-regulated in Fb7:0-
532 10 (maker-LG7-snap-gene-91.103-mRNA-1) is suspected to be associated with
533 terpenoid biosynthesis as its closest ortholog in *A. thaliana*, (MYC2_ARATH) has also
534 been related to sesquiterpene biosynthesis (Hong *et al.* 2012). Until now, TF were not
535 related to VOC in fruits.

536

537 In addition, it should be mentioned that there were 114 differentially expressed genes
538 whose function could not be assigned by sequence similarity. Therefore, we cannot
539 discard these genes may be involved in the volatile phenotypes (Supplemental Table 5).

540

541 SNPs between NILs Fb5:0-35 and Fb7:0-10

542 Although none of the accessions used in this work has been sequenced, the interspecific
543 nature of the NILs is likely to provide a high number of polymorphisms between the
544 introgressed regions (from *F. bucharica* FDP601) and the recurrent parental (*F. vesca*
545 var. 'Reine des Vallées'). The RNAseq results presented here constitute **the first**
546 transcriptome for these accessions and therefore the first global view of the genetic
547 divergence at SNP resolution between them. The transcriptome of the introgressed
548 region of NIL Fb5:0-35 had 6,813 polymorphisms (6,622 SNPs and 191 indels), and
549 Fb7:0-10 10,850 polymorphisms (10,517 SNPs and 333 indels) with respect to RV
550 (Table 6). A detailed list of the SNP polymorphisms and position is given in
551 Supplemental Table 7.

552

553 **Discussion**554 Volatile profile particularities of the diploid strawberry

555 Woodland strawberry (*F. vesca*) aroma is known to have significant qualitative and
556 quantitative differences when compared with commercial varieties (*F. x ananassa*)
557 (Ulrich *et al.* 2007). *F. vesca* fruit produce higher levels of esters and terpenoids and a
558 more intense aroma, besides the production of specific compounds such as methyl 2-
559 aminobenzoate (aka methyl anthranilate) that confers the characteristic 'wild
560 strawberry' aroma (Ulrich *et al.* 2007). In this study we profiled the volatile
561 composition of a NIL collection derived from an inter-specific cross between *F. vesca*
562 and *F. bucharica* (Urrutia *et al.* 2015). The genetic background of *F. vesca* confers
563 stability and homogeneity to the collection with outstanding organoleptic quality, but
564 the homozygous introgressions of *F. bucharica*, an exotic relative of *F. vesca*, confer
565 important phenotypic variability that can be used to map QTL for agronomical and
566 metabolic traits (Urrutia *et al.* 2015a; Urrutia *et al.* 2016). The alleles of *F. bucharica*
567 usually had a negative effect on the volatile compounds, as there was a decrease in level
568 of most of the volatiles mapped QTL.

569

570 The total number of identified volatile compounds was higher in this *F. vesca* NIL
571 collection (100) than in previous studies with *F. x ananassa* populations (81 in
572 Schwiterman *et al.* (2014) and 87 in Zorrilla-Fontanesi *et al.* (2012)). The *F. vesca* NIL
573 collection volatile profiling revealed a very complex composition. One hundred of the
574 compounds produced were identified, the majority of them being esters (46%), followed
575 by aldehydes (16%), ketones (14%), alcohols (11%), and several terpenoids, furans and
576 lactones (13%). These proportions are in agreement with that described in other studies
577 with octoploid strawberries (Schwiterman *et al.* 2014, Zorrilla-Fontanesi *et al.* 2012).
578 All the compounds identified in the *F. vesca* NIL collection have been previously
579 described in strawberry fruit, and around 20 of them have been reported to be important
580 for its aroma (Latrasse 1991; Schieberle & Hofmann 1997; Ulrich *et al.* 1997; Ulrich *et*
581 *al.* 2007).

582

583 The identified compounds that were not found in octoploid studies correspond to esters
584 such as methyl 2-aminobenzoate, methyl acetate, methyl cinnamate, methyl 3-
585 hydroxyoctanoate, ethyl methylthioacetate and 2,3-butanediol diacetate, and to
586 terpenoids such as α -farnesene and α -pinene (Zorrilla-Fontanesi *et al.* 2012) that might

587 contribute to the special aroma of wild strawberry. We also identified nerolidol and
588 linalool segregating within our collection. These compounds have been reported to be
589 characteristic of octoploid *Fragaria* species and produced by a truncated allele of the
590 *FaNES* gene (Aharoni *et al.* 2004; Chambers *et al.* 2012). However we found a clear
591 QTL at LG3:0-8 cM (Figure 5) for the accumulation of these two compounds that co-
592 locates with the *FaNES* gene. The *F. vesca* RV parental does not produce linalool or
593 nerolidol, but they were both detected in the hybrid (analyzed only in 2013;
594 Supplemental Table 1). This suggests that the *F. bucharica* alleles for the *FaNES* gene
595 produce linalool and nerolidol. Both parentals in the NIL collection (*F. vesca* and *F.*
596 *bucharica*), the F₁ hybrid and the lines in the collection producing linalool and nerolidol
597 (Fb3:0-8 and Fb3:0-15), together with a *F. x ananassa* as a positive control, were
598 genotyped for *FaNES* alleles following the method described by Aharoni *et al.* (2004).
599 The conclusion from the observed results is that the truncated *FaNES* allele is absent in
600 our collection (data not shown). This suggests that there may be several alleles
601 producing linalool in strawberry and that some of them may have arisen before
602 octoploidization.

603

604 Volatilome comparison between *F. vesca* RV and YW

605 *F. vesca* YW is a white fruited strawberry known to have a pleasant, intense fruity
606 aroma with tropical (pineapple-like) notes. Used in this study as an out-group of the
607 NIL collection, it had a different pattern of volatile accumulation, enriched in esters and
608 with higher accumulation ratios than *F. vesca* RV (Figure 1). A recent study with the
609 white fruited octoploid species *F. chiloensis*, also known for its intense, tropical fruity
610 aroma, reported that the characteristic tropical fruit aroma came from a set of six esters,
611 two of which, ethyl hexanoate (49) and hexyl acetate (52), we detected as associated to
612 *F. vesca* YW (Figure 3). The other four compounds (furfuryl acetate, acetyl acetate, 1-
613 methylethyl dodecanoate and ethyl tetradecanoate) were not detected under our
614 experimental conditions. They may be absent in and only detected in other *Fragaria sp.*
615 or failed to be detected by our volatile profiling method (Prat *et al.* 2014).

616

617 Volatile QTL in strawberry

618 Significant year to year correlation was detected for most compounds (82 out of 100)
619 although the correlation index and the significance threshold varied considerably. The
620 correlation values reported here are higher than those reported for volatile compounds in

621 other studies (Eduardo *et al.* 2013). Differences in the relative volatile accumulation
622 pattern in each NIL in the two studied harvests appear to be mainly associated to their
623 genotypes (Figure 4) and to a lower extent to the environment. This is in contrast to
624 what has been reported in other studies with octoploid strawberry (Forney *et al.* 2000;
625 Zorrilla-Fontanesi *et al.* 2012) and peach (*Prunus persica*) (Eduardo *et al.* 2013;
626 Sanchez *et al.* 2014), where the effect of the environment was more relevant. The
627 special configuration of our mapping population, as near isogenic lines, may be
628 responsible for such stability, avoiding epistatic effects among different QTL. The fact
629 that all lines share a common genetic background, in contrast to other mapping
630 populations where genetic differences between lines is wider, may highlight the effect
631 of the genotype, caused by exotic introgressions, and buffer the effect of the
632 environment over the phenotypic traits, as all lines may respond in a similar way. In
633 fact, stability of the lines has been previously proved with a (poly)-phenolic profiling of
634 the NIL collection (Urrutia *et al.* 2016), and although the correlation between genotypes
635 according to volatile profiling is lower, the median of all genotypes is above 0.70.

636

637 QTL mapping revealed 50 major stable QTL that accounted for a high proportion of the
638 variability of 47 compounds, including 14 major QTL identified for 13 KVCs: (E)-2-
639 hexenal, (Z)-3-hexenal, (E)-2-hexenyl acetate, (Z)-3-hexenyl acetate, butyl butanoate,
640 methyl-2-aminobenzoate (2), methyl butanoate, methyl cinnamate, methyl hexanoate,
641 myrtenyl acetate, mesifurane, linalool and nerolidol. Many of the QTL cluster in a few
642 genetic regions, suggesting that the compounds are co-regulated and controlled by a
643 reduced number of loci. LG5 and LG7 seem to be the most determinant regions
644 controlling volatile compounds synthesis as they accumulate the largest number of QTL
645 and harbor nine and two major QTL for KVCs, respectively. Some of the detected
646 QTLs were in agreement with those described by Zorrilla-Fontanesi *et al.* (2012) as
647 they co-locate according to synteny studies (Rousseau-Gueutin *et al.* 2008, Tennessen *et*
648 *al.* 2014). A QTL for methyl benzoate was located at LG1:26-61 cM in *F. vesca* and at
649 LGI-F.1: 38 cM in *F. x ananassa*. A QTL for benzyl acetate was located at LG7:0-
650 10 cM in *F. vesca* and at LGVII-F.1c: 9 cM in *F. x ananassa*. A QTL for ethyl
651 decanoate was mapped to LG3:8-15 cM for *F. vesca*, and to LGIII-F.1: 4 cM and LGIII-
652 M.1: -8 cM in *F. x ananassa*. A QTL for mesifurane was located at LG7:27-43 cM in *F.*
653 *vesca*, and to LGVII-F.2: 18 cM and LGVII-M.2:65 cM in *F. x ananassa*. The latter

654 QTL is associated with the *FaOMT* gene responsible for its accumulation that also co-
655 locates with our QTL (Zorrilla-Fontanesi *et al.* 2012).

656

657 There were also QTLs located previously in different regions in *F. x ananassa* and *F.*
658 *vesca* and volatile compounds that showed significant variability in one population and
659 not in the other, highlighting that different genetic backgrounds and environments can
660 reveal different genetic traits. As an example of this, we found two QTLs controlling
661 the accumulation of methyl 2-aminobenzoate, which is characteristic of *F. vesca* aroma
662 and was not detected in *F. x ananassa*. Previous reports have mapped a QTL for the
663 accumulation of γ -decalactone in the homeolog LGIII-M.2: 50-54 cM (Zorrilla-
664 Fontanesi *et al.* 2012) and a candidate gene *FaFAD1* with an eQTL co-localized
665 (Sanchez-Sevilla *et al.* 2014). However, we found no significant QTL for γ -decalactone
666 in our collection. Although data suggests that there might be an increase in the
667 production of this compound in lines with introgressions at the end of LG5, this increase
668 is not enough to report a significant effect (Supplemental Table 1). However, this
669 suggests there may be other genetic regions controlling γ -decalactone accumulation in
670 *F. vesca*.

671

672 C₆ compounds from the lipoxygenase pathway and the corresponding acetate esters
673 ((*E*)-2-hexen-1-ol, (*E*)-2-hexenal, (*E*)-2-hexenyl acetate, (*Z*)-3-hexenal and (*Z*)-3-
674 hexenyl acetate) are commonly described as 'green volatile compounds' and are usually
675 considered too variable within genotypes or varieties to be used as discriminative
676 compounds (Ulrich *et al.* 1997). However, a recent studies in peach (*Prunus persica*)
677 reported stable QTLs for (*E*)-2-hexenyl acetate and (*Z*)-3-hexenyl acetate (Eduardo *et al.*
678 *et al.* 2012) and in tomato for (*Z*)-3-hexenal and (*E*)-2-hexenal (Rambla *et al.* 2016). Our
679 data revealed a high year to year correlation between these compounds (Table 1) and
680 QTLs that co-localize for all of them at LG5:50-76 cM, suggesting that these
681 compounds were stable and co-regulated under our conditions. By differential
682 expression analysis of the red ripe fruits it was possible to highlight genes differentially
683 expressed between the NILs and the recurrent parental RV, that might contribute to the
684 observed QTL. NILs Fb5:0-35 and Fb7:0-10 are interesting for further studies in fruity
685 and wild strawberry-like aroma as they harbor QTL for methyl 2-aminobenzoate and
686 several other esters. Differentially-expressed genes include terpene synthases and acyl-
687 transferases, which catalyze the main steps in terpenoid and ester formation, and

688 lipoxygenases, which participate in fatty acid degradation and consequently in FA-
689 derived volatiles.

690

691 In-depth characterization of the volatiles emitted by ripe strawberry fruit in a *F. vesca*
692 NIL mapping collection revealed a complex mixture of 100 compounds, varying in
693 relative abundance across the population presumably because of the effect of *F.*
694 *bucharica* alleles. The high genetic effect on the accumulation of many compounds (35
695 compounds >50% G effect) allowed 50 major QTL to be mapped, including 14 QTL for
696 compounds considered of extreme importance for strawberry aroma. Some, such as
697 methyl 2-aminobenzoate and mesifurane, are only rarely found in commercial varieties
698 (*F. x ananassa*) and are of great interest for breeding programs. Therefore, here we set
699 the ground for further studies on the inheritance of the woodland strawberry aroma that
700 may lead to improved aroma and marketability of new strawberry varieties. Further
701 studies for positional cloning of the QTLs in combination with reverse genetics will
702 shed light on the causal genes of the observed phenotypes.

703

704 **Author contribution statement:**

705 MU analysed the NILs collection, prepared fruit samples, did the statistical analyses,
706 prepared RNAseq samples and evaluated the DEG, in addition to writing the
707 manuscript. AG and JLR did the GC-MS analyses and participated in edition of the
708 manuscript. KA did the SNPs calling analyses. AM lead the project, participated in all
709 steps of phenotyping and in writing the manuscript.

710

711 The authors declare that they have no conflict of interest.

712

713 **Acknowledgements:**

714 This work was funded by grants AGL2010-21414 and RTA2013-00010 from the
715 Spanish Ministry of Economy and Competitiveness and through the “Severo Ochoa
716 Programme for Centres of Excellence in R&D” 2016-2019 (SEV-2015-0533)” and by
717 the CERCA Programme / Generalitat de Catalunya. MU was supported by a FPI
718 fellowship from the Spanish Ministry of Education. AG would like to thank
719 Metabolomic lab and COST action FA1106 for networking activities.

720 *Figure legends*

721 **Figure 1 Hierarchical clustering (HCA) and heatmap of volatile compounds levels.**

722 Ratio values of all studied volatile compounds per genotype are shown in the heatmap
723 on a blue (negative) to red (positive) scale. Compounds are numerically codified as
724 specified in Table 1. Genotypes include the NILs that were analyzed both years, RV and
725 YW. Top bar identifies the sample harvest year: 2012 (blue) and 2013 (green). The
726 HCA and dendrogram of volatile compounds was according to metabolite ratio
727 distances (Euclidean distance, complete linkage). Clusters are indicated with capital
728 letters in both the dendrogram and Table 1.

729 **Figure 2 Cluster network analysis (CNA).**

730 Metabolites are represented as nodes colored according to their biosynthetic pathway (if
731 known) or chemical structure as specified by the legend. Positive (green) and negative
732 (red) correlations with absolute values $>|0.5|$ are shown as links between the nodes.
733 Links representing absolute correlations $>|0.8|$ are wider the stronger they are and have
734 the maximum color saturation. Absolute correlations $<|0.8|$ are vaguer the weaker they
735 are and have the least width.

736 **Figure 3 PCA (PC1 and PC2) scores and loading plot.**

737 **A:** PCA scores plot. NIL, RV and YW are colored according to the harvest year as
738 specified in legend. **B:** loading plot Compounds are coded as specified in Table 1 and
739 colored according to their chemical family as specified in legend.

740 **Figure 4 ω^2 values.** Percentage of the observed variability attributable to each of the
741 factors: genotype (G), environment (E), their interaction (GxE) or to error.

742 **Figure 5 Volatile QTL.** Graphical representation of the major QTL mapped. QTL
743 shown were found to be significantly different (corrected p-value < 0.05) from the
744 recurrent parental (*F. vesca* RV), in the same direction, in both harvests for all the NILs
745 harboring the introgressed region, and explained around 20% of the variability
746 regarding the NIL collection. QTL names correspond to the volatile compound affected.
747 Colored bars indicate the biosynthetic pathway (if known) or the chemical structure of
748 the compound as in Figure 2. The positive or negative effect of the QTL over the ratio
749 regarding *F. vesca* RV is represented by the full or empty color bars respectively. For
750 locating the QTL, the LG and position (in cM) of the microsatellites (SSRs) used for
751 genotyping are given.

752 **Figure 6 Venn diagrams.** Venn diagram **A** depicts the number of annotated genes (a2)
753 expressed by each line. Colored ellipses represent analyzed lines (Fb5:0-35, Fb7:0-10

754 and RV). Venn diagram **B** depicts the number of differentially expressed genes detected
755 between each NIL and the recurrent parental (RV). Colored ellipses represent
756 comparisons (NIL vs. RV). Numbers in intersecting areas indicate that the genes are
757 shared between the lines/comparisons meeting in the area. Non-intersecting areas
758 indicate the number of genes that are specifically expressed/differentially expressed in a
759 line.

760 **Figure 7 Differentially expressed gene distribution (Manhattan plot).** Graphical
761 representation of all genes in their physical position (x-axis), and their associated $-\log_{10}$
762 (p-value) from the differential expression analysis (y-axis).

763

764

765

766

767

768

769

770

771

772

773

774

775

776

777 *Table legends*

778

779 **Table 1. Volatile compounds summary, and between harvests correlations.**

780 All identified compounds and their assigned number codes and clusters are presented.

781 Tentatively identified compounds are indicated with a T after the chemical name. A

782 selected set of important compounds contributing to strawberry aroma are indicated

783 with an arrow. Data are expressed as the ratio between samples and a reference. Mean

784 ratios and standard deviation (sd) were calculated for each compound in the recurrent

785 parental *F. vesca* (RV) and in the average NIL collection for 2012 and 2013 harvests.

786 The range of the ratios (min and max values) was calculated for the NIL collection in

787 both harvests. Correlation between harvests was calculated using average genotype

788 values in both years. Asterisk after the values indicate significance at different

789 thresholds: p-value <0.05 '*', p-value <0.01 '**', p-value <0.001 '***'. No significant

790 correlations are indicated by 'ns'.

791

792

793 **Table 2. QTL for volatile compounds detected in a *F. vesca* NIL collection.**

794 Detected QTL listed by compound's alphabetical order. The position of the QTL (LG

795 number followed by the start and end position in cM), the positive (up) or negative

796 (down) effect of the QTL over the metabolite's ratio compared with *F. vesca* RV, the797 NIL harboring the shorter *F. bucharica* introgression (in cM) that includes the QTL, the

798 results of the t-test (corrected p-value) and interval mapping analysis (LOD score), the

799 percentage of variance explained by the QTL regarding the NIL collection and the

800 stability of the QTL (detected in 1 or 2 harvests) are provided.

801

802 **Table 3 Differentially expressed genes (DEG) summary**

803 Number total, up- and down-regulated DEG obtained with annotation version 2 (a2) for

804 both contrasting hypothesis (NIL vs. RV).

805

806 **Table 4 Metabolic pathways affected**

807 List of known metabolic pathways related to DEG detected in each NIL using

808 MetGenMAP software.

809

810 **Table 5 Selected candidate genes**

811 List of selected DEG between genotypes (NIL vs RV) for each metabolic QTL

812

813 **Table 6 Polymorphism summary**

814

815

816

ACCEPTED MANUSCRIPT

817

818 Electronic Supplemental Material Legend**819 Supplemental table1:** Volatile compounds average values per genotype per year.

820 Average values (per genotype per harvests) of all detected volatile compounds are
821 provided. Data are expressed as the ratio between the samples and a reference sample.

822

823 Supplemental table 2. Pearson correlation values between volatile compounds for 2012
824 and 2013 independent harvests. Asterisk after the values indicate significance at
825 different thresholds: p-value <0.05 '*', p-value <0.01 '**', p-value <0.001 '***'

826

827 Supplemental Table 3. Analysis of variance (ANOVA) fitting the model G+E+GxE
828 and w² values. ANOVA was calculated for all volatile compounds independently
829 considering two factors, genotype (G) and environment (E), and their interaction (GxE).
830 The resulting parameters of the ANOVA test Sum of squares (SS), degrees of freedom
831 (df) and p-values are provided. Omega squared values (w²) were calculated from the
832 ANOVA parameters for G, E and GxE and reflect the percentage of variability
833 accounted by each one of them. The error is 1 minus the percentual variability
834 accounted by G, E and GxE.

835

836 Supplemental Table 4 RNAseq reads quality

837

838 Supplemental table 5 List of DEG for each contrasting hypothesis (NIL vs. RV). DEG
839 for each NIL are presented in ascending order of log₂(fold change).

840 a, gene id is according to *F. vesca* annotation 2 nomenclature841 b, log₂(fold change) values use as reference RV, so negative values indicate down-
842 regulation in NIL vs. RV and positive values up-regulation in NIL vs. RV843 c, best blast hit found for the DEG predicted proteins. Codes are according to
844 UniProtUK entries

845

846 Supplemental Figure 6 Go terms summary. Molecular function and Biological process
847 GO terms summary of the Differentially Expressed Genes.

848

849 Supplemental table 7 Polymorphisms. SNPs and Indels detected between
850 transcriptomes of NILs (Fb5:0-35 and Fb7:0-10) and RV.

851

852

853 **References**

- 854 Aharoni A, Giri AP, Verstappen FWA, Berteaux CM, Sevenier R, Sun ZK, Jongsma MA,
855 Schwab W & Bouwmeester HJ Gain and loss of fruit flavor compounds produced by
856 wild and cultivated strawberry species. *Plant Cell* (2004) **16**:3110-31.
- 857 Aharoni A, Keizer LCP, Bouwmeester HJ, Sun ZK, Alvarez-Huerta M, Verhoeven HA,
858 Blaas J, van Houwelingen AMML, De Vos RCH, van der Voet H, Jansen RC, Guis M,
859 Mol J, Davis RW, Schena M, van Tunen AJ & O'Connell AP Identification of the
860 SAAT gene involved in strawberry flavor biogenesis by use of DNA microarrays. *Plant*
861 *Cell* (2000) **12**:647-61.
- 862 Anders S & Huber W Differential expression analysis for sequence count data. *Genome*
863 *Biology* (2010) **11**:ppR106.
- 864 Anders S, Pyl PT & Huber W HTSeq—a Python framework to work with high-
865 throughput sequencing data. *Bioinformatics* (2015) **31**:166-9.
- 866 Aragüez I, Osorio S, Hoffmann T, Rambla JL, Medina-Escobar N, Granell A, Botella
867 MÁ, Schwab W & Valpuesta V Eugenol Production in Achenes and Receptacles of
868 Strawberry Fruits Is Catalyzed by Synthases Exhibiting Distinct Kinetics. *Plant*
869 *Physiology* (2013) **163**:946-58.
- 870 Beekwilder J, Alvarez-Huerta M, Neef E, Verstappen FWA, Bouwmeester HJ. &
871 Aharoni A Functional characterization of enzymes forming volatile esters from
872 strawberry and banana. *Plant Physiology* (2004) **135**:1865-78.
- 873 Bolger AM, Lohse M. & Usadel B Trimmomatic: a flexible trimmer for Illumina
874 sequence data. *Bioinformatics* (2014) **30**:2114-20.
- 875 Bruhn CM, Feldmann N, Garlitz C, Harwood J, Ivans E, Marshall M, Riley A, Thurber
876 D & Williamson E Consumer perceptions of quality: apricots, cantaloupes, peaches,
877 pears, strawberries, and tomatoes. *Journal of Food Quality* (1991) **14**:187-95.
- 878 Chambers A, Whitaker VM, Gibbs B, Plotto A & Folta KM Detection of the linalool-
879 producing NES1 variant across diverse strawberry (*Fragaria* spp.) accessions. *Plant*
880 *Breeding* (2012) **131**:437-43.
- 881 Chambers AH, Pillet J, Plotto A, Bai JH, Whitaker VM & Folta KM Identification of a
882 strawberry flavor gene candidate using an integrated genetic-genomic-analytical
883 chemistry approach. *BMC Genomics* (2014) **15**:217.
- 884 Darwish O, Shahan R, Liu ZC, Slovin JP & Alkharouf NW Re-annotation of the
885 woodland strawberry (*Fragaria vesca*) genome. *BMC Genomics* (2015) **16**:29.
- 886 Dong J, Zhang YT, Tang XW, Jin WM & Han ZH Differences in volatile ester
887 composition between *Fragaria x ananassa* and *F. vesca* and implications for strawberry
888 aroma patterns. *Scientia Horticulturae* (2013) **150**:47-53.
- 889 Eduardo I, Chietera G, Pirona R, Pacheco I, Troggio M, Banchi E, Bassi D, Rossini L,
890 Vecchietti A & Pozzi C Genetic dissection of aroma volatile compounds from the

- 891 essential oil of peach fruit: QTL analysis and identification of candidate genes using
892 dense SNP maps. *Tree Genetics & Genomes* (2013) **9**:189-204.
- 893 Epskamp SC, G; Cramer, AOJ; Waldorp, LJ; Schmittmann, VD; Borsboom, D Network
894 representations of relationships in data. R package version 1.2.4. (2012)
- 895 Forney CF, Kalt W & Jordan MA The composition of strawberry aroma is influenced
896 by cultivar, maturity, and storage. *Hortscience* (2000) **35**:1022-6.
- 897 García-Alcalde F, Okonechnikov K, Carbonell J, Cruz LM, Götz S, Tarazona S,
898 Dopazo J, Meyer TF & Conesa A. Qualimap: evaluating next-generation sequencing
899 alignment data. *Bioinformatics* (2012) **28**:2678-9.
- 900 Goff SA & Klee HJ Plant Volatile Compounds: Sensory Cues for Health and
901 Nutritional Value? *Science* (2006) **311**:815-9.
- 902 Granell A & Rambla JL Biosynthesis of volatile compounds. In: *The Molecular Biology*
903 *and Biochemistry of Fruit Ripening* (eds. by Seymour GB, Poole M, Giovannoni JJ &
904 Tucker GA) Blackwell Publishing Ltd, Oxford, UK. (2013) pp. 135-161.
- 905 Hong GJ, Xue XY, Mao YB, Wang LJ & Chen XY Arabidopsis MYC2 Interacts with
906 DELLA Proteins in Regulating Sesquiterpene Synthase Gene Expression. *Plant Cell*
907 (2012) **24**:2635-48.
- 908 Jetti RR, Yang E, Kurnianta A, Finn C & Qian MC Quantification of selected aroma-
909 active compounds in strawberries by headspace solid-phase microextraction gas
910 chromatography and correlation with sensory descriptive analysis. *Journal of Food*
911 *Science* (2007) **72**:S487-S96.
- 912 Joung JG, Corbett AM, Fellman SM, Tieman DM, Klee HJ, Giovannoni JJ & Fei ZJ
913 Plant MetGenMAP: An Integrative Analysis System for Plant Systems Biology. *Plant*
914 *Physiology* (2009) **151**:1758-68.
- 915 Latrasse A. Fruits III. In: *Volatile Compounds in Fruits and Beverages* (ed. by Maarse
916 H), Dekker, New York, USA. (1991) pp. 333-87.
- 917 Liao ZH, Chen M, Guo L, Gong YF, Tang F, Sun XF & Tang KX Rapid isolation of
918 high-quality total RNA from *Taxus* and *Ginkgo*. *Preparative Biochemistry &*
919 *Biotechnology* (2004) **34**:209-14.
- 920 McCarthy F, Wang N, Magee GB, Nanduri B, Lawrence M, Camon E, Barrell D, Hill
921 D, Dolan M, Williams WP, Luthe D, Bridges S & Burgess S AgBase: a functional
922 genomics resource for agriculture. *BMC Genomics* (2006) **7**:229.
- 923 Medina-Puche L, Cumplido-Laso G, Amil-Ruiz F, Hoffmann T, Ring L, Rodriguez-
924 Franco A, Caballero JL, Schwab W, Munoz-Blanco J & Blanco-Portales R MYB10
925 plays a major role in the regulation of flavonoid/phenylpropanoid metabolism during
926 ripening of *Fragaria x ananassa* fruits. *J Exp Bot* (2014) **65**:401-17.
- 927 Olbricht K, Grafe C, Weiss K & Ulrich D Inheritance of aroma compounds in a model
928 population of *Fragaria x ananassa* Duch. *Plant Breeding* (2008) **127**:87-93.

- 929 Prat L, Espinoza MI, Agosin E & Silva H Identification of volatile compounds
930 associated with the aroma of white strawberries (*Fragaria chiloensis*). *Journal of the*
931 *Science of Food and Agriculture* (2014) **94**:752-9.
- 932 Rambla JL, López-Gresa MP, Bellés JM, Granell A Metabolomic profiling of plant
933 tissues. In: *Plant Functional Genomics (Methods in Molecular Biology 1284 series)*
934 (eds. Alonso J.M. & Stepanova A.N.). Springer, New York, USA. doi: 10.1007/978-1-
935 4939-2444-8_11. (2015) pp. 221-235
- 936 Rambla JL, Medina A, Fernández-del-Carmen A, Barrantes W, Grandillo S, Cammareri
937 M, López-Casado G, Rodrigo G, Alonso A, García-Martínez S, Primo J, Ruiz JJ,
938 Fernández-Muñoz R, Monforte AJ, Granell A Identification, introgression, and
939 validation of fruit volatile QTLs from a red-fruited wild tomato species. *J Exp Bot*
940 (2016) **68**: 429-442.
- 941 RCoreTeam R: A language and environment for statistical computing. R Foundation for
942 Statistical Computing, Vienna, Austria. (2012)
- 943 Rousseau-Gueutin M, Lerceteau-Köhler E, Barrot L, Sargent DJ, Monfort A, Simpson
944 D, Arús P, Guérin G & Denoyes-Rothan B Comparative Genetic Mapping Between
945 Octoploid and Diploid *Fragaria* Species Reveals a High Level of Colinearity Between
946 Their Genomes and the Essentially Disomic Behavior of the Cultivated Octoploid
947 Strawberry. *Genetics* (2008) **179**:2045-60.
- 948 RStudio RStudio: Integrated development environment for R RStudio, Boston, MA,
949 USA. (2012)
- 950 Sanchez-Sevilla JF, Cruz-Rus E, Valpuesta V, Botella MA & Amaya I Deciphering
951 gamma-decalactone biosynthesis in strawberry fruit using a combination of genetic
952 mapping, RNA-Seq and eQTL analyses. *BMC Genomics* (2014) **15**:218.
- 953 Sanchez G, Martinez J, Romeu J, Garcia J, Monforte AJ, Badenes ML & Granell A The
954 peach volatilome modularity is reflected at the genetic and environmental response
955 levels in a QTL mapping population. *BMC Plant Biology* (2014) **14**:137.
- 956 Schieberle P & Hofmann T Evaluation of the character impact odorants in fresh
957 strawberry juice by quantitative measurements and sensory studies on model mixtures. *J*
958 *Agric Food Chem* (1997) **45**:227-32.
- 959 Schwab W, Davidovich-Rikanati R & Lewinsohn E Biosynthesis of plant-derived flavor
960 compounds. *The Plant Journal* (2008) **54**:712-32.
- 961 Schwieterman ML, Colquhoun TA, Jaworski EA, Bartoshuk LM, Gilbert JL, Tieman
962 DM, Odabasi AZ, Moskowitz HR, Folta KM, Klee HJ, Sims CA, Whitaker VM &
963 Clark DG Strawberry Flavor: Diverse Chemical Compositions, a Seasonal Influence,
964 and Effects on Sensory Perception. *PLoS ONE* (2014) **9**:e88446.
- 965 Shulaev V, Sargent DJ, Crowhurst RN, Mockler TC, Folkerts O, Delcher AL, Jaiswal P,
966 Mockaitis K, Liston A, Mane SP, Burns P, Davis TM, Slovin JP, Bassil N, Hellens RP,
967 Evans C, Harkins T, Kodira C, Desany B, Crasta OR, Jensen RV, Allan AC, Michael
968 TP, Setubal JC, Celton J-M, Rees DJG, Williams KP, Holt SH, Rojas JJR, Chatterjee
969 M, Liu B, Silva H, Meisel L, Adato A, Filichkin SA, Troggio M, Viola R, Ashman T-L,
970 Wang H, Dharmawardhana P, Elser J, Raja R, Priest HD, Bryant DW, Fox SE, Givan

- 971 SA, Wilhelm LJ, Naithani S, Christoffels A, Salama DY, Carter J, Girona EL, Zdepski
972 A, Wang W, Kerstetter RA, Schwab W, Korban SS, Davik J, Monfort A, Denoyes-
973 Rothan B, Arus P, Mittler R, Flinn B, Aharoni A, Bennetzen JL, Salzberg SL,
974 Dickerman AW, Velasco R, Borodovsky M, Veilleux RE & Folta KM The genome of
975 woodland strawberry (*Fragaria vesca*). *Nat Genet* (2011) **43**:109-16.
- 976 Tennessen JA, Govindarajulu R, Ashman TL & Liston A Evolutionary origins and
977 dynamics of octoploid strawberry subgenomes revealed by dense targeted capture
978 linkage maps. *Genome Biol Evol* (2014) **6**:3295-313.
- 979 Trapnell C, Williams BA, Pertea G, Mortazavi A, Kwan G, van Baren MJ, Salzberg SL,
980 Wold BJ & Pachter L Transcript assembly and quantification by RNA-Seq reveals
981 unannotated transcripts and isoform switching during cell differentiation. *Nature*
982 *biotechnology* (2010) **28**:511-518.
- 983 Ulrich D, Hoberg E, Rapp A & Kecke S Analysis of strawberry flavour - discrimination
984 of aroma types by quantification of volatile compounds. *Zeitschrift Fur Lebensmittel-*
985 *Untersuchung Und-Forschung a-Food Research and Technology* (1997) **205**:218-23.
- 986 Ulrich D, Komes D, Olbricht K & Hoberg E Diversity of aroma patterns in wild and
987 cultivated *Fragaria* accessions. *Genetic Resources and Crop Evolution* (2007) **54**:1185-
988 96.
- 989 Urrutia M, Bonet J, Arús P & Monfort A A near-isogenic line (NIL) collection in
990 diploid strawberry and its use in the genetic analysis of morphologic, phenotypic and
991 nutritional characters. *Theoretical and Applied Genetics* (2015) **128**:1261-75.
- 992 Urrutia M, Schwab W, Hoffmann T & Monfort A Genetic dissection of the
993 (poly)phenol profile of diploid strawberry (*Fragaria vesca*) fruits using a NIL collection.
994 *Plant Science* (2016) **242**:151-168.
- 995 Zorrilla-Fontanesi Y, Rambla JL, Cabeza A, Medina JJ, Sánchez-Sevilla JF, Valpuesta
996 V, Botella MA, Granell A & Amaya I Genetic Analysis of Strawberry Fruit Aroma and
997 Identification of O-Methyltransferase FaOMT as the Locus Controlling Natural
998 Variation in Mesifurane Content. *Plant Physiology* (2012) **159**:851-70.
- 999

ACCEPTED MANUSCRIPT

1001

ACCEPTED MANUSCRIPT

1002

1003 **Table 1** Volatile compounds summary and between harvests correlations.

KV C	Code	Compound	Pathway	Cluster	Family	Correlation		Recurrent parental (RV)				NIL collection								
						corr.	sig.	2012		2013		2012			2013					
								mean	sd	mean	sd	mean	sd	range	mean	sd	range			
	1	1-decanol		A	alcohol	0,9	**	1,24	0,8	0,93	0,51	0,60	1,1	0,0	5,43	0,60	0,78	0,0	3,61	
	2	1-hexanol	Fatty Acid Deriv.	C	alcohol	-	ns	1,05	0,2	1,05	0,67	1,29	0,9	0,4	6,87	1,24	0,68	0,3	3,92	
	3	1-octanol		D2	alcohol	0,78	**	1,73	0,9	1,01	0,48	0,72	0,7	0,0	3,51	0,67	0,52	0,0	2,19	
	4	1-penten-3-ol		C	alcohol	0,33	ns	1,26	0,6	0,89	0,46	1,30	0,8	0,2	6,15	1,15	0,45	0,2	2,45	
	5	2-heptanol		D2	alcohol	0,72	**	1,42	1,3	1,00	0,48	0,71	1,0	0,0	4,53	0,46	0,56	0,0	4,13	
	6	2-nonanol		D2	alcohol	0,83	***	1,34	1,10	1,08	0,47	0,66	0,84	0,00	4,03	0,51	0,48	0,01	1,89	
	7	2-tridecanol		D2	alcohol	0,62	***	1,36	1,11	1,16	1,06	0,95	1,18	0,05	7,57	0,63	0,77	0,02	4,04	
	8	2-undecanol		D2	alcohol	0,78	***	1,25	0,76	1,18	0,87	0,77	0,92	0,04	5,21	0,53	0,48	0,03	1,87	
	9	(E)-2-hexen-1-ol	Fatty Acid Deriv.	B	alcohol	0,82	***	1,08	0,35	0,82	0,48	1,36	1,56	0,02	7,41	1,08	0,90	0,01	4,35	
	10	Ethanol		A	alcohol	0,41	*	0,80	0,65	0,39	0,21	1,09	1,70	0,01	7,26	0,68	1,07	0,02	6,00	
	11	Eugenol	Benzoid	D2	alcohol	0,81	***	0,42	0,14	0,94	0,94	0,88	2,45	0,05	19,2	1,08	2,93	0,04	19,19	
	12	3,4-dimethylbenzaldehyde	Benzoid	C	aldehyde	0,42	*	1,02	0,24	0,97	0,10	1,01	0,49	0,42	3,03	0,97	0,20	0,52	2,35	
	13	Benzaldehyde	Benzoid	C	aldehyde	0,78	***	1,05	0,26	1,01	0,28	1,35	0,85	0,31	5,58	1,17	0,54	0,31	2,73	
	14	Decanal		C	aldehyde	-0,01	ns	1,00	0,24	0,99	0,36	0,88	0,23	0,39	1,49	1,02	0,35	0,47	1,85	
	15	(E)-2-decenal		D2	aldehyde	0,57	**	1,16	0,42	0,74	0,27	1,16	0,46	0,26	2,58	0,95	0,75	0,13	6,22	
	16	(E)-2-heptenal		C	aldehyde	0,90	***	1,30	0,40	1,17	0,68	3,14	4,85	0,26	24,0	8	3,23	4,23	0,19	19,28
→	17	(E)-2-hexenal	Fatty Acid Deriv.	C	aldehyde	0,88	***	1,32	0,18	1,03	0,30	1,11	0,40	0,24	1,85	1,07	0,40	0,31	1,83	
	18	(E)-2-nonenal		C	aldehyde	0,47	*	0,63	0,15	0,96	0,29	0,68	0,21	0,24	1,26	0,99	0,42	0,27	2,29	

19	(E)-2-octenal		C	aldehyde	0,52	**	1,73	0,84	1,10	0,34	1,40	0,67	0,35	3,61	1,18	0,48	0,25	2,80	
20	(E)-2-pentenal		C	aldehyde	0,58	**	1,88	1,10	1,75	1,60	2,32	1,60	0,15	8,63	2,19	1,33	0,30	7,13	
21	(E,Z)-2,4-heptadienal		C	aldehyde	0,34	ns	1,27	0,45	1,00	0,46	1,13	0,56	0,52	3,89	1,12	0,50	0,37	3,87	
22	Heptanal		C	aldehyde	0,54	**	1,28	0,55	1,29	0,74	1,20	0,57	0,51	3,51	1,51	0,91	0,42	4,88	
23	Hexanal	Fatty Acid Deriv.	C	aldehyde	0,62	**	1,18	0,21	1,02	0,40	1,27	0,36	0,45	2,35	1,27	0,36	0,46	2,34	
24	Nonanal		C	aldehyde	0,09	ns	1,30	0,61	1,60	0,74	1,30	0,70	0,39	4,92	1,28	0,79	0,43	4,69	
25	Octanal		C	aldehyde	0,41	*	2,32	1,45	3,38	3,30	2,81	2,58	0,27	17,0	3	2,91	3,07	0,31	14,83
26	Pentanal		C	aldehyde	0,12	ns	1,24	0,49	1,55	0,89	1,41	0,70	0,25	3,27	1,57	0,81	0,31	4,49	
→ 27	(Z)-3-hexenal	Fatty Acid Deriv.	C	aldehyde	0,94	***	1,23	0,31	1,40	0,86	2,67	3,17	0,50	15,0	3	4,08	5,62	0,52	25,13
28	1-methylbutyl butanoate		D2	ester	0,76	***	1,91	3,33	1,79	1,19	0,72	1,21	0,07	7,41	0,74	1,61	0,13	12,17	
29	1-methylethyl butanoate		D2	ester	0,16	ns	2,11	1,94	1,50	0,83	1,24	0,91	0,25	4,23	0,68	0,66	0,04	3,58	
30	1-methylethyl acetate		C	ester	0,00	ns	1,27	0,64	0,58	0,28	1,48	0,73	0,27	3,56	0,74	0,48	0,11	2,57	
31	1-methylhexyl acetate		D2	ester	0,31	ns	1,24	1,16	0,93	0,53	1,02	1,51	0,00	8,69	0,47	0,57	0,01	3,73	
32	1-methyloctyl butanoate		D2	ester	0,68	***	0,78	0,54	1,33	0,61	0,56	0,84	0,06	4,76	0,63	0,96	0,05	6,13	
33	2,3-butanedioldiacetate T		A	ester	0,75	***	0,70	0,65	0,33	0,29	1,24	2,36	0,04	12,9	1	0,74	1,53	0,01	9,07
34	2-methylbutyl acetate		C	ester	0,60	**	1,25	0,51	0,76	0,35	1,65	0,93	0,42	5,28	0,88	0,59	0,19	3,16	
35	3-methyl-2-butenyl acetate		C	ester	0,62	**	1,33	0,51	0,87	0,43	1,57	1,27	0,18	7,26	1,20	1,05	0,17	5,58	
36	3-methylbutyl acetate		C	ester	0,27	ns	1,44	0,46	0,32	0,10	1,26	0,88	0,02	6,92	0,69	0,54	0,10	3,16	
37	Benzyl acetate	Benzoid	D1	ester	0,75	***	2,51	1,54	1,54	1,04	1,31	1,09	0,13	4,82	1,16	0,91	0,08	3,97	
→ 38	Butyl acetate		D2	ester	0,25	ns	1,08	0,43	0,93	0,28	1,38	1,14	0,13	4,96	0,98	0,79	0,08	4,04	
→ 39	Butyl butanoate		D2	ester	0,63	***	1,13	0,62	1,74	0,96	0,88	1,31	0,02	6,87	1,06	1,47	0,01	7,66	
40	Butyl hexanoate		A	ester	0,77	***	1,12	0,73	1,21	0,53	0,71	1,01	0,02	4,99	1,11	1,71	0,01	9,21	
41	Cinnamyl acetate	Benzoid	D1	ester	0,67	***	1,13	0,49	1,90	2,14	1,40	2,79	0,02	19,8	4	0,61	0,81	0,01	3,75
42	Decyl acetate		A	ester	0,88	***	1,03	0,50	0,85	0,45	0,52	0,85	0,01	4,53	0,57	0,68	0,01	2,85	
→ 43	(E)-2-hexenyl acetate	Fatty Acid Deriv.	B	ester	0,92	***	3,13	1,06	0,75	0,44	1,25	0,85	0,00	4,08	1,01	1,06	0,01	5,46	
44	Ethyl 2-hexenoate		A	ester	0,65	***	0,59	0,63	0,69	0,32	1,15	2,20	0,01	11,6	3	0,67	1,04	0,02	6,22

45	Ethyl acetate		A	ester	0,54	**	1,27	1,49	0,43	0,22	1,61	3,18	0,01	17,7	5	0,58	0,69	0,01	2,96
→ 46	Ethyl butanoate		D2	ester	0,56	**	1,59	1,20	1,15	0,72	0,96	1,04	0,01	4,08	0,82	0,64	0,01	3,11	
47	Ethyl decanoate		A	ester	0,77	***	0,67	0,61	0,37	0,23	0,74	1,65	0,00	7,41	0,58	1,83	0,01	12,59	
48	Ethyl dodecanoate		A	ester	0,79	***	0,80	1,10	0,28	0,18	1,26	3,24	0,01	17,0	3	0,80	3,38	0,01	23,06
→ 49	Ethyl hexanoate		A	ester	0,68	***	1,22	0,94	1,17	0,61	0,61	0,87	0,00	3,18	0,59	0,57	0,01	2,39	
50	Ethyl methylthioacetate		D2	ester	0,35	ns	2,76	2,35	1,25	0,64	1,18	1,54	0,03	5,78	1,39	1,18	0,02	5,19	
51	Ethyl octanoate		A	ester	0,76	***	1,13	1,08	0,75	0,43	0,69	1,29	0,00	4,72	0,54	1,10	0,01	6,84	
→ 52	Hexyl acetate		D2	ester	0,52	**	1,47	0,51	1,26	0,35	1,02	0,58	0,16	2,64	1,00	0,61	0,12	3,34	
53	Hexyl butanoate		D2	ester	0,72	***	1,02	0,79	1,26	0,65	0,80	1,09	0,03	4,63	1,15	1,75	0,01	10,46	
54	Hexyl hexanoate		D2	ester	0,63	***	0,91	0,47	1,45	1,03	0,67	0,84	0,02	3,89	1,03	1,29	0,01	7,17	
→ 55	Methyl 2-aminobenzoate		D2	ester	0,84	***	0,77	0,27	1,85	1,72	1,37	1,25	0,01	5,90	1,26	1,96	0,01	13,03	
56	Methyl 2-hexenoate		D2	ester	0,44	*	2,07	1,23	1,18	0,74	1,60	2,54	0,12	15,5	6	0,85	0,97	0,08	4,92
57	Methyl 3-hydroxyoctanoate T		D2	ester	0,54	**	1,89	0,86	2,41	2,09	0,89	1,07	0,00	11,1	6,15	0,90	1,04	0,01	8,18
58	Methyl acetate T		D2	ester	-0,01	ns	1,78	1,65	0,72	0,37	1,88	1,63	0,23	6	0,90	0,67	0,07	4,40	
59	Methyl benzoate	Benzoid	D1	ester	0,74	***	1,67	1,11	0,75	0,44	1,17	1,19	0,10	7,01	1,15	1,32	0,05	7,10	
→ 60	Methyl butanoate		D2	ester	0,49	*	2,09	1,75	1,29	0,88	1,01	1,12	0,04	6,96	0,82	0,81	0,01	3,67	
→ 61	Methyl cinnamate T	Benzoid	D1	ester	0,71	***	0,75	0,50	0,45	0,28	1,65	1,82	0,01	11,1	6	1,34	2,61	0,02	22,49
62	Methyl decanoate		D2	ester	0,86	***	1,07	0,49	0,80	0,51	0,78	0,75	0,01	3,07	0,70	0,84	0,01	4,73	
63	Methyl dodecanoate		A	ester	0,87	***	1,25	1,20	0,72	0,53	0,88	1,49	0,09	6,59	0,65	1,49	0,04	9,76	
→ 64	Methyl hexanoate		D2	ester	0,81	***	1,27	0,92	1,21	0,73	0,69	0,80	0,01	3,20	0,82	0,80	0,02	3,46	
65	Methyl octanoate		D2	ester	0,81	***	1,29	0,52	0,78	0,47	0,88	0,70	0,05	2,81	0,69	0,65	0,01	3,09	
→ 66	Myrtenyl acetate		D2	ester	0,74	***	1,94	0,69	1,51	0,70	1,12	0,57	0,23	3,25	0,96	0,69	0,17	4,73	
67	Nonyl acetate		D2	ester	0,59	**	1,11	0,39	1,27	0,88	0,96	0,67	0,20	2,95	0,92	0,95	0,20	4,88	
68	Octyl acetate		A	ester	0,79	***	1,41	0,69	1,08	0,54	0,61	0,79	0,01	3,29	0,58	0,54	0,01	2,48	
69	Octyl butanoate		A	ester	0,68	***	1,04	0,81	1,03	0,54	0,50	1,09	0,03	6,19	0,84	1,39	0,02	9,86	

	70	Octyl hexanoate	A	ester	0,77	***	1,71	1,16	1,49	0,95	0,51	1,27	0,03	7,89	0,74	1,25	0,02	8,75		
	71	Pentyl acetate	C	ester	0,30	ns	1,46	0,41	0,78	0,15	1,25	0,56	0,47	3,03	0,93	0,59	0,13	3,87		
	72	Propyl butanoate	D2	ester	0,48	*	1,21	0,52	0,98	0,46	1,12	1,16	0,03	5,24	0,91	0,85	0,02	3,77		
→	73	(Z)-3-hexenyl acetate	Fatty Acid Deriv.	C	ester	0,80	***	1,31	0,82	0,71	0,43	1,38	1,79	0,17	10,2	0	1,85	2,83	0,09	22,01
	74	2,1-pentenylfuran	C	furan	0,72	***	1,64	0,56	1,05	0,42	1,40	0,79	0,08	4,08	1,26	0,63	0,13	2,79		
	75	2-pentylfuran	C	furan	0,61	**	1,14	0,23	0,88	0,21	1,31	0,59	0,22	2,89	1,14	0,40	0,47	2,49		
→	76	Furaneol	D1	furan	-0,27	ns	1,73	1,22	0,81	1,02	1,58	1,78	0,02	9,65	3,20	7	0,01	120,6	4	
→	77	Mesifurane	D1	furan	0,69	***	1,59	0,79	0,28	0,20	1,48	1,12	0,05	5,43	0,31	0,28	0,01	1,23		
	78	1-penten-3-one	C	ketone	0,54	**	1,74	0,56	1,63	0,30	1,84	0,97	0,31	4,47	1,36	0,60	0,36	3,20		
	79	2-heptanone	D2	ketone	0,67	***	1,39	0,68	1,45	0,65	0,80	0,71	0,02	3,66	0,86	0,52	0,01	2,55		
	80	2-nonanone	D2	ketone	0,83	***	1,24	0,53	1,42	0,68	0,77	0,69	0,00	3,39	0,79	0,51	0,01	2,01		
	81	2-pentadecanone	A	ketone	0,71	***	2,03	2,39	1,46	1,45	0,99	1,44	0,02	6,32	0,72	1,06	0,01	5,06		
	82	2-pentanone	D2	ketone	0,76	***	1,55	0,98	1,63	0,75	0,82	1,18	0,01	6,73	0,83	0,72	0,01	3,62		
	83	2-tridecanone	D2	ketone	0,64	***	1,27	0,77	1,05	0,84	0,73	0,76	0,01	4,06	0,57	0,55	0,01	2,62		
	84	2-undecanone	D2	ketone	0,66	***	1,26	0,58	1,32	0,97	0,91	0,83	0,02	4,32	0,71	0,51	0,02	2,35		
	85	4-tridecanone	D2	ketone	0,76	***	1,26	1,10	1,37	1,08	1,17	1,33	0,48	9,58	1,10	0,95	0,45	5,27		
	86	6-methyl-5-hepten-2-one	C	ketone	0,63	***	0,85	0,31	1,00	0,38	1,06	0,46	0,29	2,46	1,37	0,44	0,35	2,82		
	87	Acetone	C	ketone	0,74	***	1,46	0,60	0,94	0,57	1,08	0,66	0,13	3,43	0,79	0,44	0,08	2,02		
	88	Acetophenone	Benzoid	D1	ketone	0,76	***	1,68	0,65	1,35	0,70	1,11	0,77	0,07	3,34	1,04	1,21	0,09	10,73	
	89	α -ionone	D2	ketone	0,51	**	1,67	0,58	1,63	1,19	1,39	1,17	0,16	5,31	1,19	0,90	0,21	4,91		
	90	β -ionone	D2	ketone	0,55	**	1,48	0,64	0,88	0,40	1,26	0,68	0,23	3,46	0,98	0,43	0,13	1,98		
	91	(Z)-geranyl acetone	D2	ketone	0,32	ns	1,08	0,56	0,98	0,40	1,09	0,57	0,19	3,10	1,09	0,43	0,29	2,57		
→	92	γ -decalactone	D2	lactone	0,75	***	2,05	1,25	14,31	5	0,96	1,59	0,01	37,5	10,3	11,7	0,01	119,9	6	
	93	α -farnesene	Terpenoids	D2	terpenoid	0,55	**	1,72	1,84	1,60	1,06	1,27	1,36	0,04	6,96	1,01	1,01	0,14	6,68	
	94	α -pinene	Terpenoids	C	terpenoid	0,76	***	1,10	0,41	0,61	0,23	1,45	0,86	0,32	4,14	1,11	1,03	0,14	6,00	
	95	Limonene	Terpenoids	C	terpenoid	0,31	ns	1,25	0,52	0,79	0,34	1,05	0,78	0,36	5,54	0,86	0,32	0,34	1,89	

				d															
→	96	Linalool	Terpenoids	C	terpenoi d	0,78	***	1,06	0,33	0,72	0,35	1,32	1,44	0,25	9,92	1,70	1,98	0,31	11,65
	97	Myrtenol	Terpenoids	C	terpenoi d	0,64	***	1,88	0,48	0,78	0,29	1,10	0,64	0,17	3,18	0,98	1,06	0,17	7,86
	98	Nerol	Terpenoids	C	terpenoi d	0,84	***	1,40	0,36	0,77	0,21	1,08	0,71	0,05	3,61	1,21	1,12	0,01	5,88
→	99	Nerolidol	Terpenoids	C	terpenoi d	0,95	***	1,00	0,00	1,00	0,00	1,24	0,94	1,00	6,73	1,20	0,77	1,00	5,83
	100	Terpineol	Terpenoids	C	terpenoi d	0,25	ns	1,25	0,36	1,04	0,31	1,18	0,40	0,43	2,33	1,20	0,68	0,30	3,80

1004

1005

1006

1007

1008

1009 **Table 2** QTL for volatile compounds detected in a *F. vesca* NIL collection.

	Compound	direction	qtl (cM)	shorter NIL	t-test (corrected p.value)	LOD	% explained variance	stable
	(E)-2-decenal	down	LG7:0-26	Fb7:0-27	<0,05	4.64	46%	1
	(E)-2-decenal	down	LG7:27-59	Fb7:0-59	<0,05	6.14	56%	1
	(E)-2-heptenal	down	LG7:0-10	Fb7:0-10	<0,05	2.10	25%	1
	(E)-2-heptenal	up	LG5:50-76	Fb5:50-76	<0,05	15.17	46-87%	2
	(E)-2-hexen-1-ol	down	LG5:50-76	Fb5:50-76	<0,05	15.66	63-88%	2
→	(E)-2-hexenal	down	LG5:50-76	Fb5:50-76	<0,05	16.04	74-88%	2
→	(E)-2-hexenyl acetate	down	LG5:50-76	Fb5:50-76	<0,05	16.75	82-89%	2
	(E)-2-nonenal	down	LG5:50-76	Fb5:50-76	<0,05	4.59	46%	1

	(E)-2-octenal	down	LG7:52-59	Fb7:52-59	<0,05	2.61	30%	1
	(E)-2-pentenal	down	LG7:0-10	Fb7:0-10	<0,05	2.91	30-32%	2
→	(Z)-3-hexenal	up	LG5:50-76	Fb5:50-76	<0,05	14.76	58-86%	2
→	(Z)-3-hexenyl acetate	up	LG5:50-76	Fb5:50-76	<0,05	5.68	44-53%	2
	1-decanol	down	LG5:0-11	Fb5:0-11	<0,05	1.86	16-22%	2
	1-decanol	down	LG3:8-15	Fb3:0-15	<0,05	<1,80	2-5%	2
	1-decanol	down	LG4:20-44	Fb4:0-44	<0,05	<1,80	1-5%	2
	1-hexanol	up	LG5:50-76	Fb5:50-76	<0,05	1.99	23%	1
	1-methylbutyl butanoate	down	LG5:11-35	Fb5:0-35	<0,05	<1,80	10-11%	2
	1-methylbutyl butanoate	down	LG7:0-10	Fb7:0-10	<0,05	<1,80	2-3%	2
	1-methylhexyl acetate	down	LG4:9-44	Fb4:0-44	<0,05	2.68	30%	1
	1-methyloctyl butanoate	down	LG2:0-30	Fb2:0-30	<0,05	<1,80	7-13%	2
	1-methyloctyl butanoate	down	LG5:11-35	Fb5:0-35	<0,05	<1,80	17-21%	2
	1-octanol	down	LG1:26-61	Fb1:26-61	<0,05	<1,80	1-3%	2
	1-octanol	down	LG2:0-30	Fb2:0-30	<0,05	<1,80	10-16%	2
	1-octanol	down	LG5:11-35	Fb5:0-35	<0,05	<1,80	5-17%	2
	1-penten-3-ol	down	LG7:0-10	Fb7:0-10	<0,05	5.25	51%	1
	1-penten-3-one	down	LG7:0-10	Fb7:0-10	<0,05	3.97	42%	1
	2,1-pentenyl furan	down	LG7:0-10	Fb7:0-10	<0,05	4.45	36-45%	2
	2,3-butanedioldiacetate T	up	LG7:0-10	Fb7:0-10	<0,05	2.49	6-28%	2
	2-heptanol	down	LG4:9-44	Fb4:0-44	<0,05	1.94	23%	1
	2-methylbutyl acetate	down	LG7:43-59	Fb7:43-59	<0,05	<1,80	7-8%	2
	2-nonanol	down	LG1:26-61	Fb1:26-61	<0,05	<1,80	1%	2
	2-nonanol	down	LG5:11-35	Fb5:0-35	<0,05	<1,80	13-15%	2
	2-nonanol	down	LG4:9-44	Fb4:0-44	<0,05	4.95	48%	1
	2-nonanone	down	LG4:9-44	Fb4:0-44	<0,05	6.48	58%	1
	2-pentanone	down	LG4:9-44	Fb4:0-44	<0,05	2.09	25%	1

	2-pentylfuran	down	LG7:0-10	Fb7:0-10	<0,05	3.16	35%	1
	2-pentylfuran	up	LG2:0-30	Fb2:0-30	<0,05	3.16	21-35%	2
	2-tridecanol T	down	LG3:8-15	Fb3:0-15	<0,05	<1,80	3-17%	2
	2-undecanol T	down	LG4:20-44	Fb4:0-44	<0,05	<1,80	1-15%	2
	2-undecanol T	down	LG5:11-35	Fb5:0-35	<0,05	<1,80	18-20%	2
	2-undecanone T	down	LG4:20-44	Fb4:0-44	<0,05	<1,80	2-31%	2
	3-methyl-2-butenyl acetate	up	LG3:54-94	Fb3:54-94	<0,05	2.07	11-24%	2
	3-methyl-2-butenyl acetate	up	LG2:39-45	Fb2:39-47	<0,05	5.54	5-49%	2
	3-methylbutyl acetate	up	LG3:54-94	Fb3:54-94	<0,05	3.29	36%	1
	acetone	down	LG4:9-44	Fb4:0-44	<0,05	2.24	26%	1
	acetone	up	LG5:50-76	Fb5:50-76	<0,05	2.99	33%	1
	acetophenone	down	LG3:54-94	Fb3:54-94	<0,05	1.80	14-21%	2
	acetophenone	down	LG4:0-20	Fb4:0-20	<0,05	<1,80	6-15%	2
	acetophenone	down	LG6:101-101	Fb6:101-101	<0,05	<1,80	14-20%	2
	acetophenone	down	LG7:0-10	Fb7:0-10	<0,05	<1,80	8-19%	2
	a-farnesene	down	LG4:20-44	Fb4:0-44	<0,05	2.29	10-26%	2
	a-farnesene	down	LG3:8-15	Fb3:0-15	<0,05	<1,80	16%	2
	a-ionone	down	LG1:26-61	Fb1:26-61	<0,05	3.35	16-36%	2
	a-pinene	up	LG5:0-11	Fb5:0-11	<0,05	4.20	35-42%	2
	benzaldehyde	up	LG2:0-30	Fb2:0-30	<0,05	<1,80	13-19%	2
	benzyl acetate	down	LG7:0-10	Fb7:0-10	<0,05	2.26	15-26%	2
	benzyl acetate	down	LG6:101-101	Fb6:101-101	<0,05	<1,80	18-21%	2
	b-ionone	down	LG1:26-61	Fb1:26-61	<0,05	2.58	18-30%	2
→	butyl acetate	up	LG1:26-61	Fb1:26-61	<0,05	<1,80	6-15%	2
→	butyl butanoate	down	LG5:11-35	Fb5:0-35	<0,05	3.51	30-38%	2
→	butyl butanoate	down	LG7:0-10	Fb7:0-10	<0,05	<1,80	1-2%	2
	butyl hexanoate	down	LG5:0-11	Fb5:0-11	<0,05	3.26	30-35%	2

	butyl hexanoate	down	LG2:0-30	Fb2:0-30	<0,05	<1,80	19-20%	2
	butyl hexanoate	up	LG7:0-10	Fb7:0-10	<0,05	<1,80	11-14%	2
	cinnamyl acetate	down	LG3:54-94	Fb3:54-94	<0,05	<1,80	5-8%	2
	cinnamyl acetate	down	LG7:0-10	Fb7:0-10	<0,05	<1,80	4-6%	2
	decanal	up	LG4:0-20	Fb4:0-20	<0,05	2.51	29%	1
	decyl acetate	down	LG5:11-35	Fb5:0-35	<0,05	1.80	20-22%	2
	decyl acetate	down	LG4:20-44	Fb4:0-44	<0,05	<1,80	1-16%	2
	ethanol	up	LG7:0-10	Fb7:0-10	<0,05	3.36	36%	1
	ethyl 2-hexenoate	down	LG5:11-35	Fb5:0-35	<0,05	<1,80	15-18%	2
→	ethyl butanoate	down	LG7:0-10	Fb7:0-10	<0,05	<1,80	3-10%	2
	ethyl decanoate	down	LG1:26-61	Fb1:26-61	<0,05	<1,80	2-4%	2
	ethyl decanoate	up	LG7:0-10	Fb7:0-10	<0,05	3.59	10-38%	2
	ethyl dodecanoate	down	LG2:0-30	Fb2:0-30	<0,05	<1,80	4-15%	2
	ethyl dodecanoate	up	LG7:0-10	Fb7:0-10	<0,05	3.57	5-38%	2
→	ethyl hexanoate	down	LG1:26-61	Fb1:26-61	<0,05	<1,80	1-3%	2
	ethyl methylthioacetate T	down	LG7:0-10	Fb7:0-10	<0,05	1.84	1-22%	2
	ethyl octanoate	down	LG1:26-61	Fb1:26-61	<0,05	<1,80	1-4%	2
	ethyl octanoate	up	LG7:0-10	Fb7:0-10	<0,05	3.19	10-35%	2
	eugenol	up	LG5:50-76	Fb5:50-76	<0,05	4.44	33-45%	2
	hexanal	up	LG3:54-94	Fb3:54-94	<0,05	<1,80	6-7%	2
	hexyl butanoate	down	LG5:11-35	Fb5:0-35	<0,05	4.55	34-46%	2
	hexyl butanoate	down	LG7:0-10	Fb7:0-10	<0,05	<1,80	1%	2
	hexyl hexanoate	down	LG2:0-30	Fb2:0-30	<0,05	3.53	27-38%	2
	limonene	down	LG7:0-10	Fb7:0-10	<0,05	2.03	21-24%	2
→	linalool	up	LG3:0-8	Fb3:0-8	<0,05	6.64	54-59%	2
→	mesifurane	down	LG7:26-43	Fb7:26-45	<0,05	7.27	16-62%	2
→	methyl 2-aminobenzoate T	down	LG7:0-10	Fb7:0-10	<0,05	2.54	8-29%	2

→	methyl 2-aminobenzoate T	down	LG5:11-35	Fb5:0-35	<0,05	6.79	33-60%	2
	methyl 2-hexenoate	down	LG5:11-35	Fb5:0-35	<0,05	3.26	14-35%	2
	methyl 3-hydroxyoctanoate T	down	LG3:8-15	Fb3:0-15	<0,05	<1,80	4-6%	2
	methyl benzoate	down	LG3:54-94	Fb3:54-94	<0,05	<1,80	10-11%	2
	methyl benzoate	down	LG6:101-101	Fb6:101-101	<0,05	<1,80	13-15%	2
	methyl benzoate	down	LG7:0-10	Fb7:0-10	<0,05	<1,80	11-21%	2
	methyl benzoate	up	LG1:26-61	Fb1:26-61	<0,05	<1,80	14-18%	2
→	methyl butanoate	down	LG5:11-35	Fb5:0-35	<0,05	2.79	16-31%	2
→	methyl butanoate	down	LG7:0-10	Fb7:0-10	<0,05	<1,80	1-19%	2
→	methyl cinnamate T	up	LG2:0-30	Fb2:0-30	<0,05	2.81	18-32%	2
	methyl decanoate	down	LG5:0-11	Fb5:0-11	<0,05	2.49	24-28%	2
	methyl decanoate	down	LG4:9-44	Fb4:0-44	<0,05	2.71	31%	1
	methyl dodecanoate	down	LG1:26-61	Fb1:26-61	<0,05	<1,80	1%	2
	methyl dodecanoate	down	LG2:0-30	Fb2:0-30	<0,05	<1,80	8-18%	2
	methyl dodecanoate	down	LG5:11-35	Fb5:0-35	<0,05	<1,80	13-14%	2
	methyl dodecanoate	up	LG7:0-10	Fb7:0-10	<0,05	2.80	31%	1
→	methyl hexanoate	down	LG5:11-35	Fb5:0-35	<0,05	5.54	35-52%	2
	methyl octanoate	down	LG5:0-11	Fb5:0-11	<0,05	4.83	43-48%	2
	myrtenol	down	LG7:0-10	Fb7:0-10	<0,05	4.32	8-44%	2
	myrtenol	down	LG3:8-15	Fb3:0-15	<0,05	<1,80	2-7%	2
	myrtenol	up	LG5:50-76	Fb5:50-76	<0,05	6.71	60%	1
→	myrtenyl acetate	down	LG5:11-35	Fb5:0-35	<0,05	4.67	45-47%	2
→	myrtenyl acetate	down	LG6:101-101	Fb6:101-101	<0,05	<1,80	1%	2
	nerol	down	LG4:9-20	Fb4:0-20	<0,05	4.40	17-45%	2
	nerol	down	LG7:43-59	Fb7:43-59	<0,05	<1,80	7-11%	2
	nerol	up	LG5:50-76	Fb5:50-76	<0,05	4.33	38-44%	2
→	nerolidol	up	LG3:0-8	Fb3:0-8	<0,05	22.38	76-95%	2

nonanal	down	LG7:43-59	Fb7:43-59	<0,05	5.16	50%	1
octanal	down	LG7:43-59	Fb7:43-59	<0,05	2.85	32%	1
octyl acetate	down	LG5:11-35	Fb5:0-35	<0,05	2.40	25-27%	2
octyl butanoate	down	LG2:0-30	Fb2:0-30	<0,05	2.11	21-25%	2
octyl hexanoate	down	LG2:0-30	Fb2:0-30	<0,05	1.95	21-23%	2
octyl hexanoate	down	LG1:26-61	Fb1:26-61	<0,05	<1,80	1-2%	2
octyl hexanoate	down	LG5:0-11	Fb5:0-11	<0,05	<1,80	13-20%	2
pentyl acetate	up	LG1:26-61	Fb1:26-61	<0,05	1.99	8-23%	2
propyl butanoate	down	LG7:0-10	Fb7:0-10	<0,05	2.81	5-31%	2
propyl butanoate	up	LG1:26-61	Fb1:26-61	<0,05	<1,80	7-13%	2

1010

1011

1012

1013

1014 **Table 3** Differentially expressed genes (DEG) summary

NIL vs. RV	Introgression size (Mb)	a2			
		DEG	blast homologies	Up regulated	Down regulated
Fb5:0-35	6.51	257	218	106	151
Fb7:0-10	14.20	442	367	204	234

1015

1016

1017

1018

1019

ACCEPTED MANUSCRIPT

1020

1021 **Table 4** Metabolic pathways affected

NIL vs. RV	pathway	p-value
Fb5:0-35	glutathione biosynthesis	1.51E-02
Fb5:0-35	β -alanine biosynthesis I	1.58E-02
Fb5:0-35	farnesene biosynthesis	2.22E-02
Fb5:0-35	cis-zeatin biosynthesis	2.26E-02
Fb5:0-35	linalool biosynthesis	3.41E-02
Fb5:0-35	g-glutamyl cycle	4.48E-02
Fb7:0-10	valine degradation I	7.67E-03
Fb7:0-10	divinyl ether biosynthesis II (13-LOX)	1.89E-02
Fb7:0-10	13-LOX and 13-HPL pathway	1.89E-02
Fb7:0-10	asparagine degradation I	3.38E-02
Fb7:0-10	homogalacturonan degradation	4.82E-02

1022

1023

1024

1025

1026

1027

1028

1029

1030 **Table 5** Selected candidate genes

1031

comparison vs. RV	gene id ^a	log ₂ (fold change) ^b	p-value	p-adjusted	blast hit ^c	blast hit protein description	predicted function in reference annotation (a1)
Fb5:0-35	maker-LG4-augustus-gene-138.110-mRNA-1	-Inf	1.76E-10	6.05E-08	PAT1_ARATH	Scarecrow-like transcription factor PAT1	
Fb5:0-35	mrna09934.1-v1.0-hybrid	-11.82	4.56E-44	8.49E-40	F4JBC7_ARATH	HXXXD-type acyl-transferase-like protein	Vinorine synthase (probable)
Fb5:0-35	maker-LG4-snap-gene-135.249-mRNA-1	-2.09	2.79E-05	3.74E-03	STPS1_SANAL	Sesquiterpene synthase	(+)-delta-cadinene synthase isozyme A (D-cadinene synthase A) (probable)
Fb5:0-35	augustus_masked-LG6-processed-gene-175.2-mRNA-1	1.62	5.65E-04	4.81E-02	EIF3C_ARATH	Eukaryotic translation initiation factor 3 subunit C	
Fb5:0-35	mrna32494.1-v1.0-hybrid	1.68	6.21E-04	5.20E-02	GL3_ARATH	Transcription factor GLABRA 3	Transcription factor GLABRA 3 (bHLH 1) (putative)
Fb5:0-35	maker-LG4-augustus-gene-136.257-mRNA-1	3.97	2.44E-12	9.39E-10	MFS_MENPI	(+)-menthofuran synthase	
Fb7:0-10	maker-LG7-snap-gene-1.135-mRNA-1	-Inf	5.34E-04	2.88E-02	F4KGA3_ARATH	Putative PHD finger transcription factor	
Fb7:0-10	maker-LG7-snap-gene-129.164-mRNA-1	-Inf	7.03E-08	8.53E-06	ZDH22_ARATH	Protein S-acyltransferase 24	
Fb7:0-10	snap_masked-LG7-processed-gene-42.93-mRNA-1	-7.15	2.77E-09	4.07E-07	VRN1_ARATH	B3 domain-containing transcription factor VRN1	
Fb7:0-10	mrna23606.1-v1.0-hybrid	-6.85	1.24E-14	3.45E-12	LOX2_ORYSJ	Linoleate 9S-lipoxygenase 2	3-deoxy-manno-octulosonate cytidyltransferase (CKS) (similar to)
Fb7:0-10	augustus_masked-LG7-processed-gene-126.10-mRNA-1	-6.69	2.99E-05	2.20E-03	TA12B_ARATH	Transcription initiation factor TFIID subunit 12b	

Fb7:0-10	mrna34011.1-v1.0-hybrid	-6.02	1.38E-25	1.52E-22	F4JBC7_ARATH	HXXXD-type acyltransferase-like protein	BAHD acyltransferase At5g47980 (probable)
Fb7:0-10	maker-LG3-augustus-gene-99.141-mRNA-1	-5.22	2.93E-10	4.85E-08	HIBC1_ARATH	3-hydroxyisobutyryl-CoA hydrolase 1	3-hydroxyisobutyryl-CoA hydrolase, mitochondrial (HIB-CoA hydrolase), Precursor (probable)
Fb7:0-10	augustus_masked-LG7-processed-gene-56.12-mRNA-1	-4.02	1.56E-10	2.72E-08	LOXC2_ORYSJ	Probable lipoxygenase 8, chloroplastic	Probable lipoxygenase 8, chloroplastic, Precursor (similar to)
Fb7:0-10	maker-LG7-augustus-gene-88.90-mRNA-1	-3.90	4.37E-13	9.30E-11	HIBC1_ARATH	3-hydroxyisobutyryl-CoA hydrolase 1	3-hydroxyisobutyryl-CoA hydrolase, mitochondrial (HIB-CoA hydrolase), Precursor (probable)
Fb7:0-10	augustus_masked-LG7-processed-gene-56.13-mRNA-1	-3.51	6.02E-09	8.65E-07	LOXC2_ORYSJ	Probable lipoxygenase 8, chloroplastic	Probable lipoxygenase 8, chloroplastic, Precursor (similar to)
Fb7:0-10	augustus_masked-LG3-processed-gene-102.20-mRNA-1	-2.30	6.74E-06	5.72E-04	ERF61_ARATH	Ethylene-responsive transcription factor ERF061	
Fb7:0-10	maker-LG5-snap-gene-206.105-mRNA-1	-1.97	3.70E-05	2.70E-03	GLYC7_ARATH	Serine hydroxymethyltransferase 7	Serine hydroxymethyltransferase 2 (SHMT 2) (probable)
Fb7:0-10	maker-LG7-augustus-gene-95.135-mRNA-1	-1.79	2.12E-04	1.29E-02	VRN1_ARATH	B3 domain-containing transcription factor VRN1	
Fb7:0-10	genemark-LG7-processed-gene-22.65-mRNA-1	-1.75	1.91E-04	1.19E-02	F4JW79_ARATH	Kow domain-containing transcription factor 1	
Fb7:0-10	augustus_masked-LG6-processed-gene-175.2-mRNA-1	-1.56	1.31E-03	6.03E-02	EIF3C_ARATH	Eukaryotic translation initiation factor 3 subunit C	
Fb7:0-10	maker-LG3-augustus-gene-10.249-mRNA-1	0.44	3.61E-01	1.00E+00	ASAT1_ARATH	Acyl-CoA--sterol O-acyltransferase 1	Probable long-chain-alcohol O-fatty-acyltransferase 5
Fb7:0-10	maker-LG6-augustus-gene-341.179-mRNA-1	1.86	1.53E-03	6.87E-02	TPS10_RICCO	Terpene synthase 10	Myrcene synthase, chloroplastic, Precursor (probable)
Fb7:0-10	augustus_masked-	2.83	1.59E-	7.05E-02	ZDH14_ARATH	Probable protein S-	Probable S-acyltransferase

	LG7-processed-gene-50.27-mRNA-1		03			acyltransferase 14	At3g60800 (putative)
Fb7:0-10	maker-LG5-augustus-gene-34.145-mRNA-1	3.14	5.88E-04	3.12E-02	LOX2_ARATH	Lipoxygenase 2, chloroplastic	Lipoxygenase 2, chloroplastic (AtLOX2), Precursor (similar to)
Fb7:0-10	maker-LG7-snap-gene-91.103-mRNA-1	3.35	3.42E-05	2.50E-03	MYC2_ARATH	Transcription factor MYC2	
Fb7:0-10	maker-LG7-augustus-gene-8.110-mRNA-1	6.44	4.87E-22	2.37E-19	NAC86_ARATH	NAC domain-containing protein 86	
Fb7:0-10	mrna23453.1-v1.0-hybrid	11.01	2.67E-20	2.02E-17	O23392_ARATH	HXXXD-type acyl-transferase family protein	Vinorine synthase (probable)
Fb7:0-10	mrna34009.1-v1.0-hybrid	13.29	3.28E-39	6.22E-35	F4JBC7_ARATH	HXXXD-type acyl-transferase-like protein	Vinorine synthase (probable)
Fb7:0-10	augustus_masked-LG7-processed-gene-21.17-mRNA-1	Inf	3.17E-05	2.33E-03	HIBC1_ARATH	3-hydroxyisobutyryl-CoA hydrolase 1	

1032 ^a gene id is according to *F. vesca* annotation version 2 nomenclature

1033 ^b $\log_2(\text{fold change})$ values use as reference RV, so negative values indicate down-regulation in NIL and positive values up-regulation in NIL

1034 ^c best blast hit found for the DEG predicted proteins. Codes are according to UniProtUK entries

1035

1036

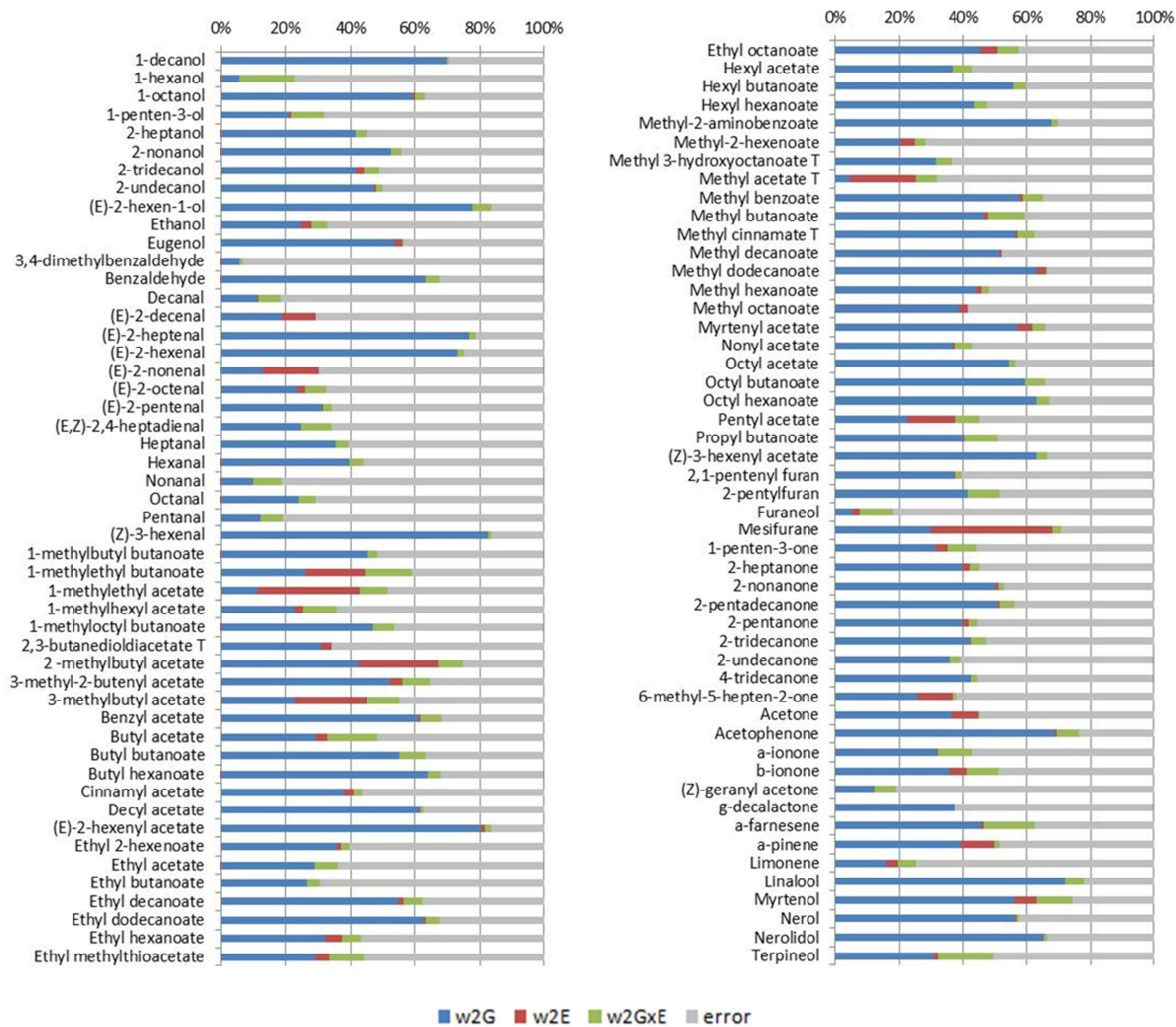
1037

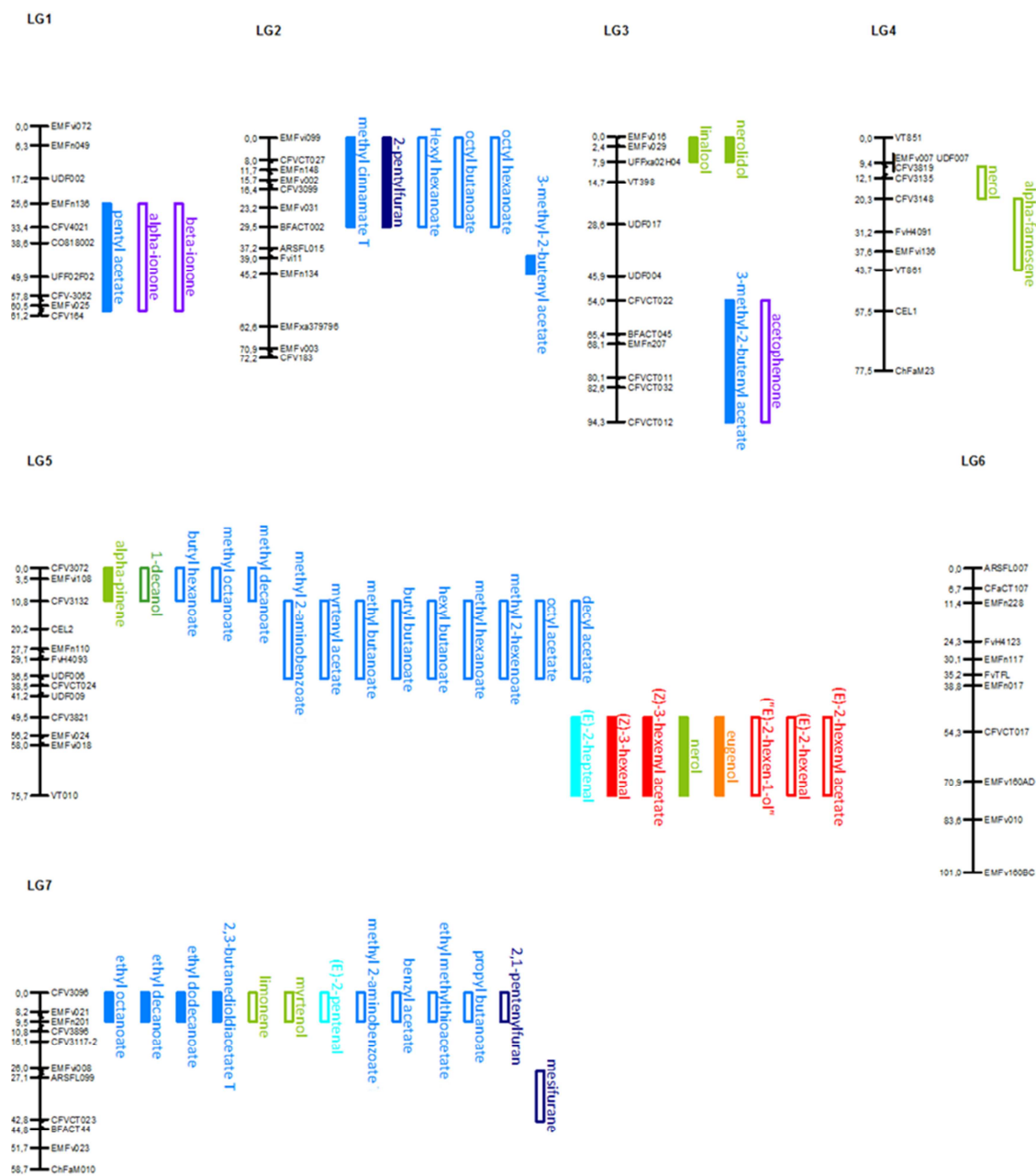
1038 **Table 6** Polymorphism summary

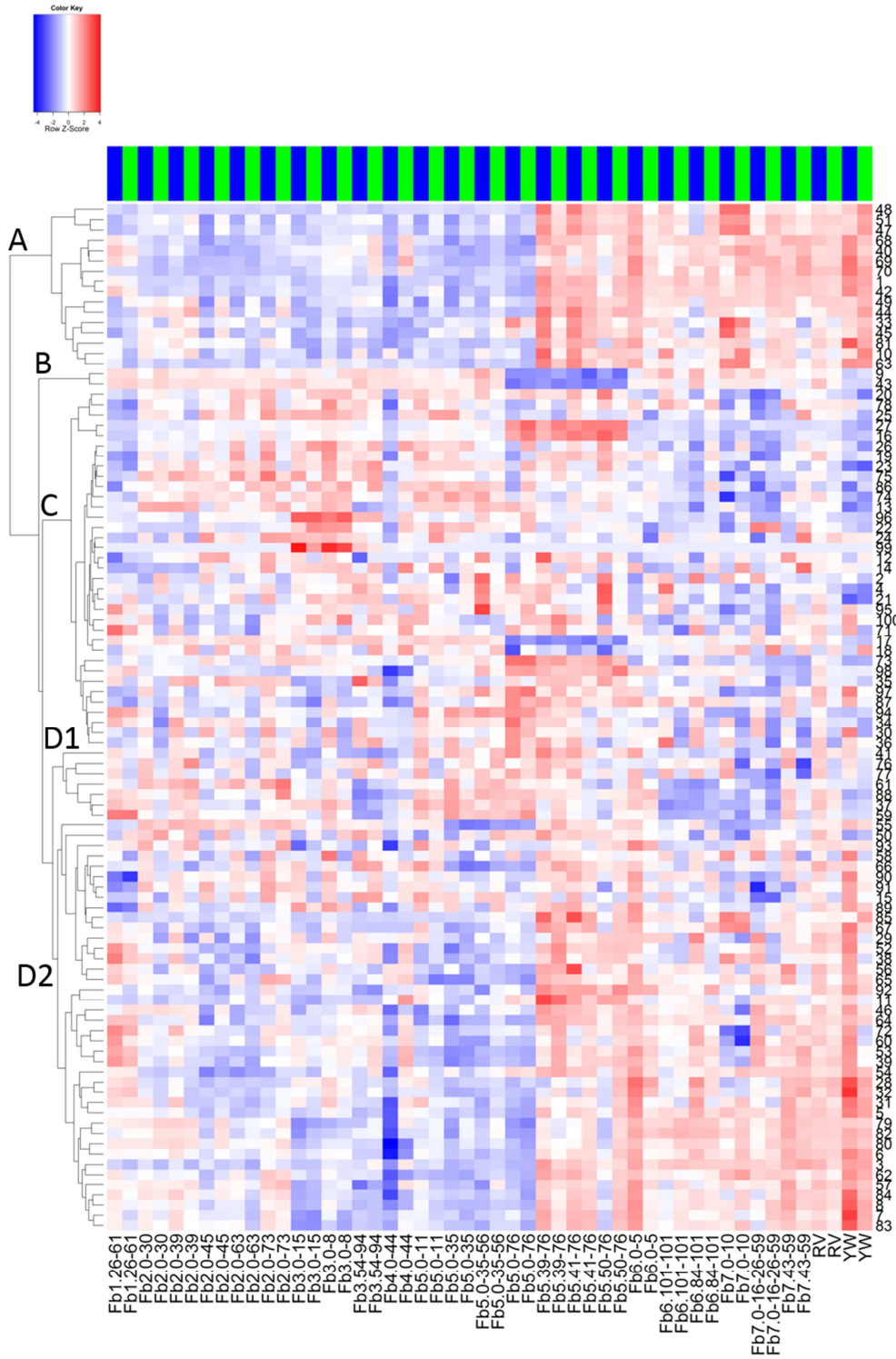
	Fb5:0-35	Fb7:0-10	total
Introgression cM	35	10	
Introgression bp	5.593.948	15.652.556	
SNPs vs. RV	6622	10517	17139
Indels vs. RV	191	333	524
total polymorphisms	6813	10850	17663

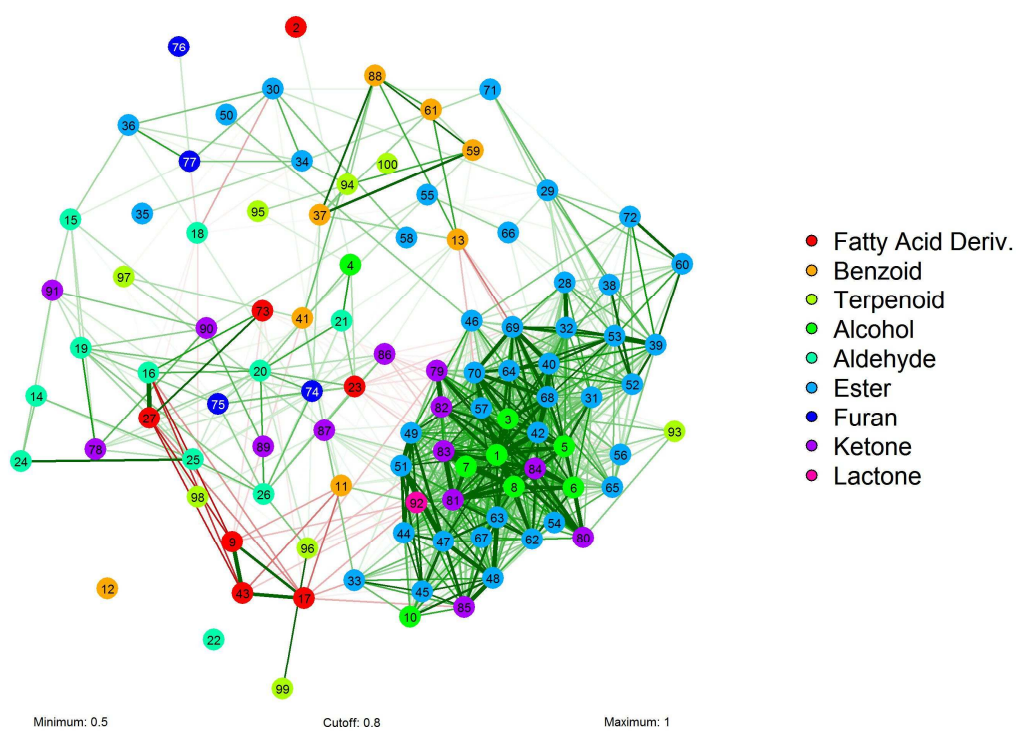
1039

1040

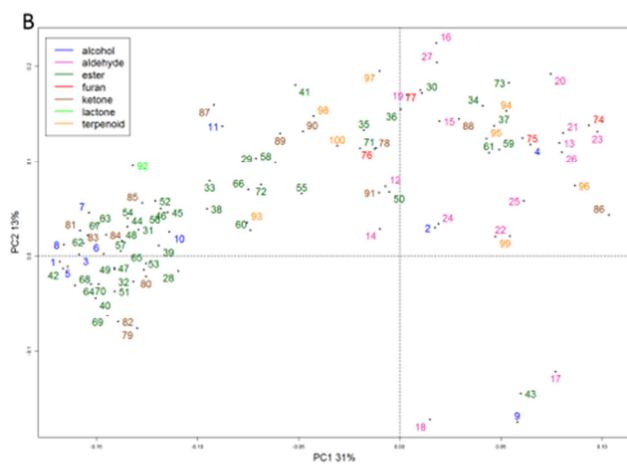
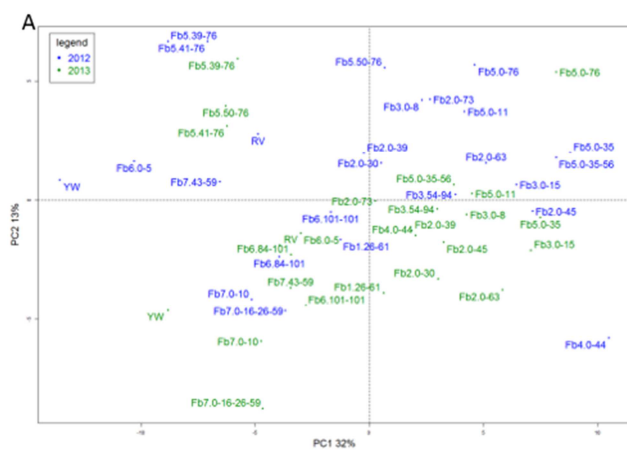


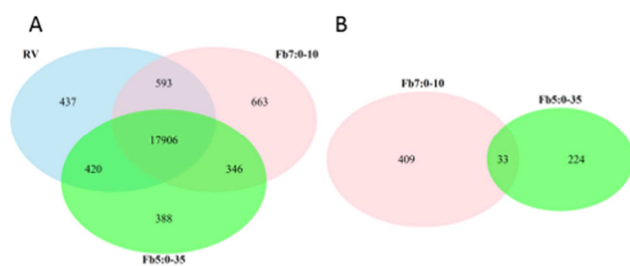


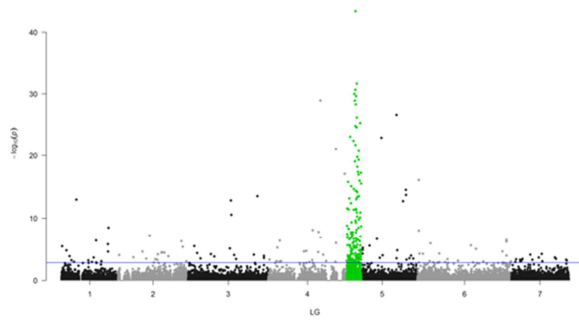
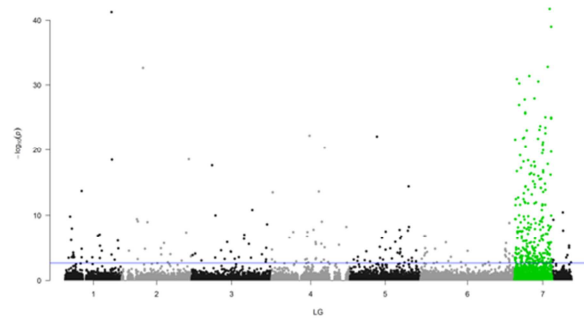




ACCEPTED M





Fb5:0-35**Fb7:0-10**

ACCEPTED MANUSCRIPT

- Volatile composition of wild strawberry as model of octoploide cultivated fruit.
- NIL collection a tool to explore genetic variability of fruit quality traits and aroma volatiles
- 50 major QTLs controlling volatile accumulation to increase wild strawberry flavour
- Two wild strawberry genome regions harbor key aroma volatile QTL
- Differences in gene expression between NILs show possible genes important to enhance aroma.

Author contribution statement:

MU analysed the NILs collection, prepared fruit samples, did the statistical analyses, prepared RNAseq samples and evaluated the DEG, in addition to writing the manuscript. AG and JLR did the GC-MS analyses and participated in edition of the manuscript. KA did the SNPs calling analyses. AM lead the project, participated in all steps of phenotyping and in writing the manuscript.

The authors declare that they have no conflict of interest.